ISSN 2782-1730

hospital

# **Medical Bulletin** of the Main Military Clinical Hospital named after N.N. Burdenko

hospitalburdenko.com



2022 №3

# 2022 №3

ISSN: 2782-1730 (PRINT) / ISSN: 2713-0711 (ONLINE)
DOI: 10.53652/2782-1730-2022-3-3

**PEER-REVIEWED**
**SCIENTIFIC AND PRACTICAL JOURNAL**
**MEDICAL BULLETIN OF THE MAIN MILITARY**
**CLINICAL HOSPITAL**
**NAMED AFTER N.N. BURDENKO**

The journal's articles are included in the independent database of the complete list of scientific papers — the Russian Science Citation Index (RSCI).
Free access policy.
Electronic versions of the published issues of the journal are available online: hospitalburdenko.com

MEDICAL BULLETIN OF THE MAIN MILITARY CLINICAL HOSPITAL NAMED AFTER N.N. BURDENKO

**Production: Publishing House Opinion Leader by order of Main Military Clinical Hospital named after academician N.N. Burdenko Russian Defense Ministry**
Phone: +7 926 317 4445

# 2022 №3


# CONTENTS

Chernavsky S.V.
Honored Doctor of the Russian Federation, DSc

# Features of clinical manifestations of coronary heart disease in patients with amiodarone-associated hypothyroidism

UDK 616.447-008.6
DOI: 10.53652/2782-1730-2022-3-3-5-10



**Chernavsky S.V.[1,2], Dorokhina A.V.[1], Artyushkevich O.V.[1], Stremoukhov A.A.[2], Kudentsova L.A.[1]**

[1] *Main Military Clinical Hospital named after academician N.N. Burdenko Russian Defense Ministry, Moscow, Russia*
[2] *Russian medical Academy of continuing professional education of the Ministry of health of the Russian Federation, Moscow, Russia*

**Abstract.** Coronary heart disease (CHD) is an acute problem of modern medicine. Primarily, it is determined by the high prevalence of the disease among the working-age population, as well as by the considerable mortality and disability associated with it. Amiodarone (Am) is the drug of choice in the treatment of cardiac arrhythmias (CA), one of the frequent and threatening manifestations of CHD. Long-term use of the drug can lead to the development of primary hypothyroidism (HT), which significantly aggravates the course of cardiovascular diseases.

***Objective.*** To assess the cardiovascular system (CVS) of CHD patients with the development of amiodarone-associated hypothyroidism (AmHT).

***Material and methods.*** Analysis of case histories of 810 patients with CHD and various CA who were taking Am for sinus rhythm control was performed. The case histories were examined and a retrospective analysis was performed on the clinical course of CHD in 28 patients with AmHT before and after the development of thyreopathy. To evaluate the state of cardiovascular system the patients' complaints, objective examination data, electrocardiography (ECG) and echocardiography (EchoCG) were assessed.

***Results.*** Long-term intake of Am by patients with CHD results in primary HT in 3.4% of cases. The formation of thyreopathy significantly affects the course of the disease. Patients show a 19.6% increase in myocardial volume indices and a 22.7% decrease in myocardial contractility, with a 30.2% increase in left ventricular myocardial mass (LVMM).

***Conclusion.*** Amiodarone-associated hypothyroidism is one of the significant complications developing in patients taking the drug for a long period of time. The formation of thyreopathy in patients with CHD significantly aggravates the course of the underlying disease, which should be taken into account when prescribing treatment and dynamic monitoring.

**Keywords:** amiodarone, coronary heart disease, hypothyroidism.

**Introduction.** Coronary heart disease (CHD) is one of the most common diseases of cardiovascular system (CVS) in all economically developed countries; it occupies the leading place among the causes of mortality, temporary and permanent disability [1, 2, 3].

The incidence of CHD at the age of 45 to 69 years is from 18 to 24,5% of cases [4, 5]. Besides, this nosology is the cause of high mortality and disability among people of working age. According to the Russian demographic yearbook (2021), the proportion of able-bodied people who died of CHD was 15.2% of the total number of deaths [6, 7].

Among the most frequent and threatening complications of CHD are cardiac rhythm disturbances (CRD) and conduction disorders, the incidence of which in patients ranges from 45 to 90% [8, 9, 10].

Currently, amiodarone (Am) is the drug of choice for the treatment of most types of CRD. The mechanism of electrophysiological action of Am combines the properties of all four major classes of antiarrhythmic drugs. It is able to inhibit βadrenoreceptors, inactivate potassium channels, fast sodium channels in cardiomyocyte membrane, has properties of calcium antagonists and peripheral vasodilators [11, 12]. Amiodarone significantly reduces total mortality by 13%, and mortality due to arrhythmia by 29%. The efficacy of the drug in patients with atrial and ventricular extrasystoles is 90%, and in patients with life-threatening arrhythmias — 41% [13, 14].

At the same time, taking the drug in some cases has a significant effect on thyroid function. Changes occurring in the thyroid status of patients receiving amiodarone for a long time are caused both by the action of iodine contained in the drug and by its structural similarity with thyroid hormones [15, 16]. In addition, amiodarone can both decrease and increase thyroid hormone production, which can lead to the development of hypothyroidism (HT) and thyrotoxicosis. The main pathogenetic mechanism of amiodarone-induced hypothyroidism (AmHT) is based on the fact that with chronic autoimmune damage and high iodine intake, the thyroid loses the ability to independently secrete thyroid hormones, resulting in reduced synthesis and the development of primary HT. In addition, excessive iodine supply to thyrocytes can lead to disruption of its organicization even if the structure of the gland is unchanged [17, 18].

The development and course of AmHT in most cases are nonspecific, under the "clinical masks" of worsening manifestations of cardiovascular disease, for the treatment of which the drug was prescribed. Combination of basic metabolic disorders with cardiovascular pathology significantly aggravates the course of the disease and worsens clinical prognosis of a patient [19, 20]. At the same time, the developing AmHT sometimes becomes a

**Table 1. Indicators of central hemodynamics**

| Indicators, unit. | CHD (n=28) | CHD+AmHT (n=28) |
|---|---|---|
| SBP, mmHg | 140,1±6,3 | 125,7±9,5*** |
| DBP, mmHg | 92,2±4,2 | 88,1±8,3** |
| MAP, mmHg | 104,1±11,7 | 101,4±6,8** |
| HR, bpm | 74,9±10,2 | 62,2±6,1** |
| SV, ml/min | 85,1±9,2 | 71,4±8,0** |
| MBV, l/min | 7,40±1,04 | 7,11±0,78* |
| Total peripheral resistance, dyn/s×cm$^{-5}$ | 1628±103 | 1447±227** |
| Specific peripheral resistance, mmHg ×m$^2$/L | 33,6±1,8 | 29,6±1,7** |
| Note. Significance of differences between groups I and II: *p<0.05; **p<0.01; ***p<0.001. | | |

**Table 2. Hemodynamic indices (according to EchoCG data)**

| Indicators, unit. | CHD (n=28) | CHD+AmHT (n=28) |
|---|---|---|
| ESS, cm | 3,3±0,3 | 3,6±0,2* |
| EDS, cm | 5,0±0,1 | 5,6±0,5* |
| ESV, ml | 55,2±11,7 | 68,1±12,4** |
| EDV, ml | 140,9±11,1 | 162,1±11,1* |
| EF, % | 66,07±10,3 | 50,09±9,1** |
| LVMM, gr | 175,11±12,04 | 228,20±13,01* |
| DT IVS, cm | 1,10±0,12 | 1,11±0,16* |
| DT LVPWS, cm | 1,1±0,02 | 1,1±0,06* |
| RV, cm | 2,13±0,13 | 2,16±0,11 |
| LA, cm | 3,62±0,13 | 3,78±0,17* |
| Note. Significance of differences between groups I and II: *p<0.05; **p<0.01; ***p<0.001. | | |

problem, which causes unreasonable refusal to prescribe Am, which can be rather dangerous when administering the drug for vital indications [21].

**Material and Methods.** The analysis of medical history of 810 patients with coronary heart disease and various CRD who received Am for sinus rhythm control for more than 6 months in the dose not less than 200 mg/day was carried out. 107 (13.2%) of those examined developed signs of amiodarone-induced thyreopathies while taking Am. In 28 (26.1%) of them AmHT was diagnosed on the basis of a characteristic clinical picture and laboratory indices [22]. Subsequently, medical histories were examined and a retrospective analysis of the clinical course of CHD in 28 AmHT patients before and after the development of thyreopathy was performed. The mean age of subjects was 65.2±1.7 years, number of males and females did not differ significantly (47.2 and 52.8%, respectively). The duration of CHD was 6–8 years. To evaluate CVS state the patients' complaints, objective examination data, electrocardiography (ECG) and echocardiography (EchoCG) with the determination of left ventricular (LV) end-diastolic size (EDS), LV end-systolic size (ESS), LV end-diastolic volume (EDV), LV end-systolic volume (ESV), stroke volume (SV), minute blood volume (MBV), ejection fraction (EF), left ventricular myocardial mass (LVMM), right ventricular (RV) and left atrial (LA) size, as well as diastolic thickness (DT) of interventricular septum (IVS) and left ventricular posterior wall (LVPWS) were assessed.

**Results.** The main complaints of CHD patients before the development of AmHT were general weakness (12.2%), edema (7.6%), dyspnea (11.1%) and decreased working capacity (23.6%). It should be noted that a number of patients (15.9%) did not have any complaints. Subsequently, in the course of thyreopathy development, the pattern of complaints changed considerably. More often an increase of unmotivated general weakness (56,2%), dyspnea (13,4%), as well as peripheral edema (12,2%) and CRD (12,2%) were noted. The revealed complaints indicate the progression of cardiovascular pathology.





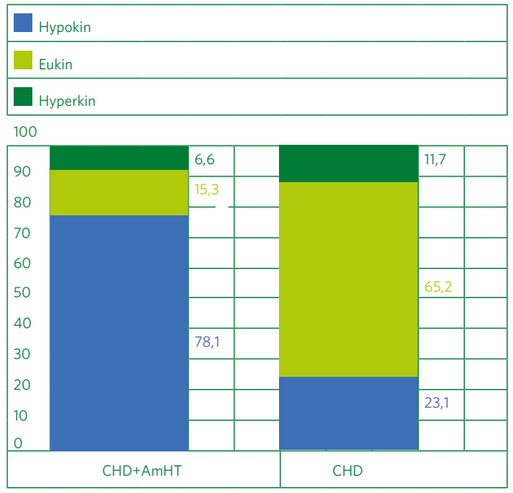


**Fig. 1.** Circulatory type in patients with CHD and AmHT (%)

The development of AmHT in CHD patients was accompanied by significant changes in cardiovascular system. The examined patients had a predisposition to arterial hypotension and bradycardia (Table 1).

Before Am administration, the majority of subjects (65.2 and 23.1%, respectively) had eu- and hypokinetic circulatory types. After AmHT manifestation, a significant number (78.1%) of patients with CHD were diagnosed with hypokinetic circulation type (Fig. 1).

The investigation of intracardiac hemodynamic indices revealed significant structural and morphological changes in myocardium in CHD patients in the course of AmHT development.

Thus, during the development of thyreopathy in CHD patients there was a significant increase in ESV and EDV by 23.6 and 15.7% on average, respectively. Similar dynamics was observed in ESS and EDS of the examined patients. The formation of AmHT was accompanied by their increase by 9.1% and 12%, respectively (Table 2).

Changes in myocardial volumetric function were accompanied by a significant decrease in myocardial contractility in the form of decreased EF by 22.7% on average. It should also be noted that the formation of AmHT in CHD patients also contributed to structural changes of myocardium. The evaluation of such parameter as LVMM revealed its increase by 30,2% on average in case of thyreopathy, at the same time there was observed an increase of DT IVS and DT LVPWS by 11 and 9,2%, respectively. The revealed significant changes of intracardiac hemodynamics during the development of AmHT are the factors of adverse course of CHD.

**Conclusions.** Primary HT develops in 3.4% of cases in CHD patients taking amiodarone for a long time. The formation of thyreopathy significantly influences the course of the disease. Patients have 19,6% increase of myocardial volume indices and 22,7% decrease of its contractility, at the same time there is 30,2% increase of LVMM.

## References

1. Russian Society of Cardiology (RSC). 2020 Clinical practice guidelines for Stable coronary artery diseasy. *Russian Journal of Cardiology.* 2020; 25(11):4076. (In Russ.). https://doi.org/10.15829/1560-4071-2020-4076
2. Genders TS, Steyerberg EW, Alkadhi H, Leschka S, Desbiolles L, Nieman K, et al. A clinical prediction rule for the diagnosis of coronary artery disease: validation, updating, and extension. *Eur Heart J.* 2011; 32(11):1316–30. https://doi.org/10.1093/eurheartj/ehr014
3. Karpov YuA, Barbarash OL, Boschenko AA, Kashtalap VV, Kukharchuk VV, Mironov VM, et al. Eurasian Guidelines for the diagnostics and management of stable coronary artery disease (2020–2021). *Eurasian heart journal.* 2021; (3):54–93. (In Russ.). https://doi.org/10.38109/2225-1685-2021-3-54-93
4. World Health Organization. SDR, ischaemic heart disease, all ages, per 1000 000. *European Health Information Gateway.* https://gateway.euro.who.int/ru/indicators/hfa_110-1340-sdr-ischaemic-heart-disease-all-ages-per-100-000/
5. Roitberg GE, Strutynsky AV. *Vnutrenniye bolezni. Serdechno-sosudistaya sistema.* Moscow: Binom-press; 2007. 346 p. (In Russ.).
6. *Demographic Yearbook of Russia 2021. Statistical collection.* Moscow: Rossta; 2021. 167 p. (In Russ.). https://rosstat.gov.ru/folder/210/document/13218
7. Karpov YuA, Sorokin EV. *Stabil'naya ishemicheskaya bolezn serdtsa: strategiya and taktika lecheniya*. 2nd ed., reprint. and additional. Moscow: Medical Information Agency; 2012. 271 p. (In Russ.).
8. Kushakovsky MS. *Aritmii serdtsa.* Saint-Petersburg: *Foliant*; 1998. 638 p. (In Russ.).
9. Miller JM, Zipes DP. *Therapy for cardiac arrhythmias*. In: Braunwald E, Zipes D, Libby P, Bonow R, eds. Heart disease. A textbook of cardiovascular medicine. Philadelphia: W.B. Saunders company; 2005. pp. 713–766.
10. Chazov EI, Bogolyubov VM. *Narusheniya ritma serdtsa.* Moscow: Meditsina; 1972. 248 p. (In Russ.).
11. Effect of prophylactic amiodarone on mortality after acute myocardial infarction and in congestive heart failure: Meta-analysis of individual date from 6500 patients in randomized trials. Amiodarone Trials Meta-Analysis Investigators. *Lancet.* 1997; 350(9089):1417–24. PMID: 9371164
12. Golitsyn SP. Amiodarone: decades of administration. *Therapeutic Archive.* 2011; 83(8):25–33. (In Russ.). URL: https://ter-arkhiv.ru/0040-3660/article/view/30881
13. Адашева Т.В., Демичева О.Ю. Кордарон и тиреоидная патология. Мифы и реальность. *Медицинский вестник.* 2013; 17:12–13. [Adasheva TV, Demicheva OY. Kordaron and thyroid pathology. Myths and reality. *Medical Bulletin.* 2013; 17:12–13. (In Russ.)].

14. Homocysteine Studies Collaboration. Homocysteine and risk of ischemic heart disease and stroke: a meta-analysis. *JAMA*. 2002; 288(16):2015–22. https://doi.org/10.1001/jama.288.16.2015
15. Gaisenok OV. The use of amiodarone in clinical practice: the problem of side effects. *Rational Pharmacotherapy in Cardiology*. 2010; 6(6):823–827. https://doi.org/10.20996/1819-6446-2010-6-6-823-827
16. Choy AM, Rankin S, Elder D, Lang CC, Ogston S, George J. 65 Incidence and Monitoring of Adverse Drug Reactions in Long-Term Amiodarone Therapy: a Retrospective Analysis in Tayside, Scotland. *Heart (British Cardiac Society)*. 2015; 101(Suppl 4):A35–A36. https://doi.org/10.1136/heartjnl-2015-308066.65
17. Sviridenko NYu, Platonova NM, Molashenko NV, Golitsyn SP, Bakalov SA, Serdyuk SE. Endocrine aspects of the use of amiodarone in clinical practice (Follow-up and treatment algorithm for patients with thyroid dysfunction). *Rossian Journal of Cardiology*. 2012; 94(2):63–71. https://doi.org/10.15829/1560-4071-2012-2-63-71
18. Dedov II, Mel'nichenko GA, Sviridenko NYu., et al. Diagnosis, treatment, and prevention of iatrogenic iodine-induced thyroid gland diseases. *Vestn Ross Akad Med Nauk*. 2006; 2:15–22. Russian. PMID: 16544899
19. Fadeev VV. Modern concepts of diagnosis and treatment of hypothyroidism in adults. Prob. *Endocrinol*. 2004; 2:47–55. (In Russ.).
20. Klein I, Ojamaa K. Thyroid hormone and the cardiovascular system. *N Engl J Med*. 2001; 344(7):501–9. https://doi.org/10.1056/NEJM200102153440707
21. Kryukov EV, Potekhin NP, Fursov AN, et al. Algorithm of management of patients receiving amiodarone, depending on the functional state of the thyroid gland. *Clinical medicine*. 2017; 95(10):901–904. (In Russ.).
22. Grineva EN, Tsoy UA, Karonova TL, Andreychenko TV, Bogdanova GA, Vanushko VE, et al. Draft of the federal clinical recommendations for diagnosisi and treatment of amiodarone-induced thyroid dysfunction. *Clinical and experimental thyroidology*. 2020; 16(2):12–24. (In Russ.). https://doi.org/10.14341/ket12693

**Information about the authors:**

**Sergej V. Chernavsky** — MD, Honored Doctor of the Russian Federation, DSc, Head of the Endocrinology Department of Main Military Clinical Hospital named after academician N.N. Burdenko Russian Defense Ministry, Moscow, Russia; Associate Professor of the Department of General Medical Practice and Outpatient Therapy, Russian medical Academy of continuing professional education of the Ministry of health of the Russian Federation, Moscow, Russia — **responsible for contacts**, **chernavskijsv@mail.ru**, ORCID: 0000-0001-5260-8761; eLibrary SPIN: 6569-4674

**Aleksandra V. Dorokhina** — MD, endocrinologist, Main Military Clinical Hospital named after academician N.N. Burdenko Russian Defense Ministry, Moscow, Russia.

**Olga V. Artyushkevich** — MD, endocrinologist, Main Military Clinical Hospital named after academician N.N. Burdenko Russian Defense Ministry, Moscow, Russia.

**Anatolij A. Stremoukhov** — MD, DSc, professor, Head of the Department of General Medical Practice and Outpatient Therapy, Russian medical Academy of continuing professional education of the Ministry of health of the Russian Federation, Moscow, Russia.

**Lyudmila A. Kudentsova** — MD, endocrinologist, Main Military Clinical Hospital named after academician N.N. Burdenko Russian Defense Ministry, Moscow, Russia.

*The authors declare no conflicts of interest.*
*The study was not sponsored.*
*Received 06.06.2022*



# Surgical mini-Scarf osteotomy in hallux valgus with biodegradable headless screws fixation

UDK 617.3
DOI: 10.53652/2782-1730-2022-3-3-11-19

**Davydov D.V., Kerimov A.A., Khominets I.V., Grechukhin D.A.**

*Main Military Clinical Hospital named after academician N.N. Burdenko Russian Defense Ministry, Moscow, Russia*

**Abstract.** The use of biodegradable implants is becoming increasingly popular, especially in operations on small bones of the skeleton, including operations on the anterior part of the foot. 23 surgical interventions were performed to correct the first metatarsal using the mini-Scarf technique and fixation of fragments with a biodegradable implant. All the operated patients did not have a severe radiological stage of osteoarthritis of the first metatarsophalangeal joint and stiffness. The results of treatment were evaluated using AOFAS and Groulier questionnaires. Out of 23 patients, it was possible to track and obtain data according to the questionnaires in 18 patients (78.3% (16 had grade III deformity (88.9%)). Six months after surgical treatment, the proportion of excellent and good results was 77.8% (14) according to the AOFAS questionnaire and 83.3% (15) according to the Groulier questionnaire. The achieved results suggest a favorable prognosis for the widespread use of magnesium oxide implants, however, further research and comparison of the results of treatment in patients with hallux valgus who underwent surgery with the use of standard titanium screws are needed.

**Keywords:** hallux valgus, magnesium, biodegradable implant, bioabsorbable implant, mini-Scarf osteotomy.

**Introduction.** PThe development of surgical treatment methods in traumatology and orthopedics and the widespread use of submersible metal structures generated the problem of their removal after achieving the required treatment result, which has not been solved at present.

Biodegradable implants have been under development since the middle of the 20th century [3–5, 9, 10]. Their use excludes repeated surgery to remove the metal structures, which not only has economic advantages, but is also much better perceived by the patients. However, according to the literature, a number of biodegradable materials do not have the required strength properties or, when implanted in vivo, lose them faster than physiological regeneration requires [5, 7–11, 13, 14]. Also, the use of biodegradable implants has significant limitations on the volume of the fixator itself. Since the body requires a certain time to "process" the implant, this material cannot be completely biologically inert, and implantation of large structures (pins and plates) can lead to undesirable reactions of body tissues in the form of aseptic inflammation or resorption [5, 7–11, 13, 14]. Therefore, relatively small pins

**Table 1. Campbell classification of transverse flatfoot**

| Signs | Degrees of deformation | | | |
|---|---|---|---|---|
| | mild | | severe | |
| Degree of transverse flatfoot | 1st | 2nd | 3rd | 4th |
| M1M2 (IMA) | 10° | 11–15° | 16–20° | >20° |
| HVA | 20° | 21–30° | 31–40° | >40° |

**Table 2. Working clinical and surgical classification of static anterior foot deformities**

| Degrees static deformation | Criteria |
|---|---|
| 1st | Visual deformity without clinically significant signs. Pain syndrome in the projection of the first "ray" of the foot is occasionally possible. Radiological signs of static deformity of the first ray of the foot: M1M2 – 10-14°; HVA – 15-20° |
| 2nd | Clinical signs of static deformity of the first "ray" of the foot only. Radiological signs of static deformity of the first ray of the foot: M1M2 – >15°; HVA – >20° |
| 3rd | Clinical signs of static deformity of the first and lateral "rays" of the foot in various combinations. Radiological signs of static deformity of the first "ray" of the foot: M1M2 – >15°; HVA – >20° |

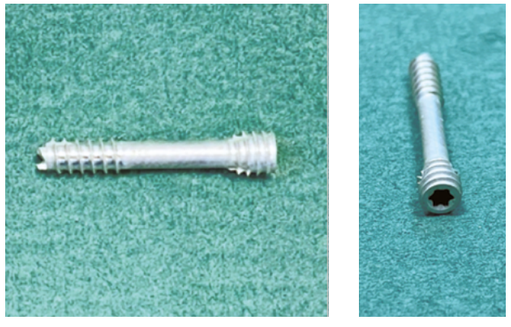

**Fig. 1.** Appearance of the MAGNEZIX® CS headless screw, 3.2 mm

and screws are most commonly used as biodegradable fixators in foot and hand surgery [1, 2, 7, 9, 10].

This article reviews our clinical experience with biodegradable implants in anterior foot surgery.

**Material and Methods.** During the period from January 2019 to December 2021, 226 patients with valgus deformity of the first toe (hallux valgus) were operated on in the Center of Traumatology and Orthopedics of the Main Military Clinical Hospital named after Burdenko. Correction of the "first ray" was performed by osteotomy of the first metatarsal bone using the mini-Scarf method with fixation via a headless cannulated screw. Titanium screws were used in 203 (89.8%) patients. Since 2020, we started to use biodegradable implants with the magnesium oxide-based implants MAGNEZIX® CS 3.2 mm (Fig. 1).

The study group included 23 female patients aged 41–63 years (mean age 53.2 years) who underwent correction of the first metatarsal bone using the mini-Scarf technique with fragment fixation by biodegradable implant.

A number of classifications were used to assess the severity of valgus deformity of the first toe.

The Campbell classification (Table 1) is based on radiological criteria and is assessed by radiographs of the anterior and medial foot in straight (dorsoplantar) projection, performed under body weight. Reliable criteria for the degree of transverse flatfoot are the parameters of angular deviation of the I metatarsal bone and the first toe. Three straight lines corresponding to the longitudinal axes of the I, II metatarsal bones and the axis of the main phalanx of the first toe are drawn on the radiographs. In the 1st degree of deformity, the angle between the I and II metatarsal bones (first intermetatarsal angle (IMA)) is 10-14°, and the angle of deviation of the first toe from the axis of the I metatarsal bone (hallux valgus angle (HVA)) is 15-20°, with the 2nd degree these angles respectively increase to 15 and 30°, with the third degree, to 20 and 40°, and with the fourth degree they exceed 20 and 40°.

However, to facilitate initial diagnosis at the stage of clinical examination of the patient, to determine indications for further advanced examination, and to simplify preoperative planning a working clinical and surgical classification (Table 2) was developed in the Center of Traumatology and Orthopedics of the Main Military Clinical Hospital named after Burdenko. This classification, based on the visual assessment of anterior foot deformity similar to the Manchester Scale, considers not only visual



**Fig. 2.** Projection of access in the area of the first metatarsophalangeal joint

**Fig. 3.** Access to the head of the metatarsal bone

examination, but also patient complaints, i.e. clinical manifestations of static deformities, and allows to diagnose static changes in the forefoot using the most noninvasive, safe, and low-cost method – the clinical examination. Visual signs of the deformity include medial convexity of the head of the first metatarsal bone and valgus deviation of the first toe. Clinical signs include persistent pain syndrome, joint contractures, corns and calluses, and toe deformities that worsen the patient's quality of life.

Among the operated patients, 16 (65.7%) had deformity of the III degree and 7 (34.3%) of the II degree. None of the operated patients had severe radiological stage of arthrosis of the first metatarsophalangeal joint and pronounced stiffness. Patients with complex foot deformities requiring surgery on several toes as well as patients with clear radiological signs of osteopenia were not included in the study group. All patients were operated on using the same technique and by the same surgeon.

***Mini-Scarf surgical technique.*** In the supine position, after applying a pneumatic tourniquet to the middle third of the thigh (pressure 250 mm Hg), we perform 3–4 cm long access in the projection of the first metatarsophalangeal joint on the anterolateral surface (Fig. 2).

Skin is sequentially dissected, the capsule of the first metatarsophalangeal joint is mobilized, from which a flap is cut out on the medial surface with the base on the main phalanx of the first toe. Access to the head of the first metatarsal bone is performed (Fig. 3).

Then, the medial exostosis of the first metatarsal bone is removed using an oscillating saw, followed by a Z-shaped distal mini-Scarf osteotomy (Fig. 4).

**Fig. 4.** The area of the Z-shaped mini-Scarf osteotomy

**Fig. 5.** Installation of the Magnezix biodegradable screw

The osteotomized distal metaepiphysis is displaced outward to the required distance and provisionally fixed with a Kirschner wire. Next, a guide pin is inserted along which a headless screw is inserted, after pre-drilling (Fig. 5). The length of the screw is determined using a special gauge and calculation, since the elements of the metal structure must not protrude beyond the bone borders.

***Postoperative rehabilitation.*** In the postoperative period, on the first and second day, the surgeon bandages the patient with a special orthopedic aseptic bandage for the forefoot. Patients walk in special unloading postoperative shoes (Baruk post-operative shoes), excluding the load on the forefoot for 4–5 weeks from the date of surgery. During this period, physical exercises are allowed only in a mild form. In 4–5 weeks after the control X-ray, the patient switches to orthopedic shoes that support the physiological arch of the foot, and begins active physical exercises and physiotherapy, aimed at the development of movements in the toe joints.

With the help of physical therapy instructors, the Main Military Clinical Hospital named after Burdenko has developed a plan for rehabilitation of patients after forefoot surgery, with each patient receiving a printed plan and exercising according to the recommendations.

***Evaluation of the treatment.*** The AOFAS (Table 3) and Groulier (Table 4) scales were used to evaluate the treatment results.

The results of treatment according to the AOFAS scale were evaluated as follows: "excellent" — 95–100 points, "good" — 75–94 points, "satisfactory" — 51–74

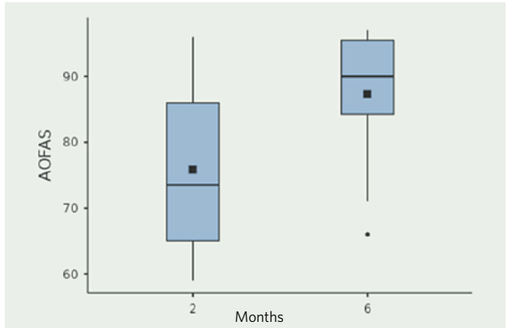


**Fig. 6.** Difference in the median of the absolute points according to AOFAS at 2 and 6 months after surgery

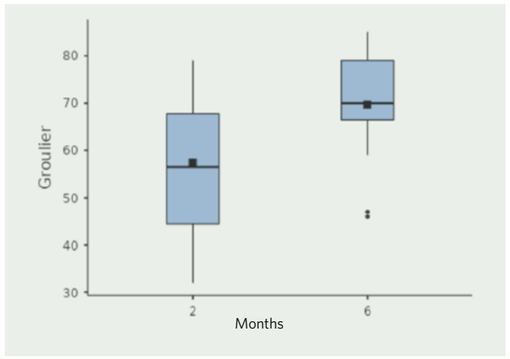


**Fig. 7.** Difference in the median of the absolute points according to Groulier at 2 and 6 months after surgery

points, and "poor" — 50 points or less. The results of the treatment on the Groulier scale were rated as follows: "excellent" — 71–85 points, "good" — 60–70 points, "satisfactory" — 29–59 points, " poor" — 28 points or less.

The AOFAS and Groulier scores were obtained after 2 and 6 months. The above time points for this period were compared by repeated measures analysis of variance. A nonparametric Friedman criterion was used to test for differences in proportions. Statistical analysis was performed using Jamovi statistical package (version 2.2.2). The $p<0.05$ value was considered statistically significant.

**Results.** When comparing the results of the surgical intervention, statistically significant improvement was noted on both the AOFAS ($\chi 2$ 16.0; df 1, $p<0.001$) and Grouilier ($\chi 2$ 18.0; df 1, $p<0.001$) questionnaires (Figures 6 and 7).The distribution of the surgical treatment results



**Table 3. AOFAS Forefoot deformity treatment outcome assessment scale**

| | | |
|---|---|---|
| **Pain (40 points)** | | |
| Painful sensations | None | 40 |
| | Mild, occasional | 30 |
| | Moderate, daily | 20 |
| | Severe, persistent | 0 |
| **Function (45 points)** | | |
| Activity limitation | No limitations of daily activity | 10 |
| | No restrictions in daily activity, only in case of overload | 7 |
| | Daily limitations, inability of overloading | 4 |
| | Limitations that exclude all activity | 0 |
| Requirement for shoes | Fashionable, comfortable, requires no insoles | 10 |
| | Comfortable, with orthopedic insoles | 5 |
| | Only specially chosen or brace | 0 |
| Movement range of the first metatarsophalangeal joint | Full or minor restriction (range 75° or more) | 10 |
| | Moderate restriction (range 30-74°) | 5 |
| | Severe restriction (range less than 30°) | 0 |
| Range of motion in the interphalangeal joint | No restrictions | 5 |
| | Severe restrictions | 0 |
| Stability in the metatarsophalangeal and interphalangeal joints | Stable | 5 |
| | Unstable or easily displaced | 0 |
| Hyperkeratoses in the joint area of the first ray | No or asymptomatic | 5 |
| | Present, painful | 0 |
| **Axis of the first ray (on examination, whether or not there is a deflection of the first finger toward the others) (15 points)** | | |
| Degree of axis recovery | Recovered | 15 |
| | Cosmetically acceptable, yet slight asymptomatic hallux valgus is present | 8 |
| | Not recovered, obvious deformity recurrence | 0 |

**Table 4.** **Groulier forefoot deformity treatment outcome assessment scale**

| | | | | | | | |
|---|---|---|---|---|---|---|---|
| Condition of 1 ray (max. 40 points) | Hallux valgus | Normal (10–20°) | 20 | Moderate (20–25°) | 15 | Recurrence or valgus deformity more than 25° | 0 |
| | Pain in the first metatarsopha langeal joint | None | 10 | Rare | 6 | Disturbing | 0 |
| | Movement in the first metatarsoph langeal joint | Normal (dorsiflexion 60–90°, plantar 0–30°) | 10 | Restricted | 6 | Stiffness | |
| Condition of the forefoot (max. 25 points) | Metatarsalgia | None | 10 | Decreased | 5 | Permanent | 0 |
| | Hyperkeratoses | None | 5 | Present | 0 | – | – |
| | Metatarsus varus | Less than 10° | 10 | 10–15° | 8 | More than 15° | 0 |
| | Shoes | Regular | 8 | Special | 6 | Other | 0 |
| Functional activity (max. 20 points) | Walking distance | No restrictions | 6 | 1 km | | Less than 500 m | 0 |
| | Activity | Sports | 6 | Professional or casual | | Decreased | 0 |

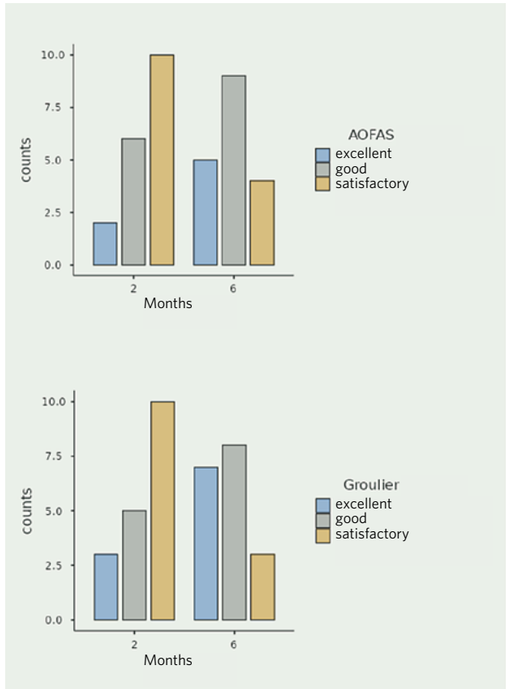


**Fig. 8.** Distribution of the results for the "excellent", "good", and "satisfactory" strata according to the AOFAS and Groulier questionnaires

after 2 and 6 months from the time of surgery is shown in Figure 8. The graph shows the distribution of the results according to the "excellent", "good", and "satisfactory" strata.

At 6 months after surgical treatment, the proportion of excellent and good results was 77.8% (14) according to the AOFAS questionnaire and 83.3% (15) according to the Groulier questionnaire.

***Clinical case.*** Patient D., born in 1958, was admitted to the hospital with the diagnosis: bilateral combined flatfoot stage III with pathological deflection of the first toes to the outside and pain syndrome. Keller's osteochondropathy of the second metatarsal bone of the left foot (Fig. 9). The radiographs of the feet before surgical treatment are shown in Fig. 10.

The patient underwent correction of the first metatarsal bone using the mini-Scarf technique with fixation of the fragments with a biodegradable implant. Postoperative radiographs (first day) are shown in Fig. 11.

**Discussion.** Despite the use of different scales, the results were largely alike. The use of biodegradable headless screws allows to achieve satisfactory and good results in most cases [2, 6]. The small sample of patients limits our observational retrospective study, however, the results obtained are consistent with larger studies published in the world literature [1, 2, 6, 10, 12].

**Conclusion.** During the study, the implant demonstrated sufficient strength, no breakage or migration of the fixator was observed. Consolidation of the first metatarsal bone was achieved in all cases. The results obtained in combination with the absence of the need for repeated surgery to remove the metal structure allow



Medical Bulletin of the Main Military Clinical Hospital named after N.N. Burdenko

**Fig. 9.** The appearance of the feet before surgery

**During the study, the implant demonstrated sufficient strength, no breakage or migration of the fixator was observed. Consolidation of the first metatarsal bone was achieved in all cases. The results obtained in combination with the absence of the need for repeated surgery to remove the metal structure allow us to make a favorable prognosis for the widespread use of magnesium oxide-based implants**

**Fig. 10.** Radiographs of the patient before surgical intervention

**Fig. 11.** Radiographs of a patient after surgical intervention on the 1st day

us to make a favorable prognosis for the widespread use of magnesium oxide-based implants. However, further studies and a comparison of the treatment results of patients with hallux valgus who were operated on using standard titanium screws are required.

## References


1. Golubev VG, Starostenkov AN. Operative technique features in application of bioabsorbable implants for limb fractures treatment. *Surgical practice.* 2017; (2):5–13. (In Russ.).
2. Atkinson HD, Khan S, Lashgari Y, Ziegler A. Hallux valgus correction utilising a modified short scarf osteotomy with a magnesium biodegradable or titanium compression screws — a comparative study of clinical outcomes. *BMC Musculoskeletal Disord.* 2019; 20(1):334. https://doi.org/10.1186/s12891-019-2717-7. PMID: 31319832
3. Cho SY, Chae SW, Choi KW, Seok HK, Kim YC, Jung JY, et al. Biocompatibility and strength retention of biodegradable Mg-Ca-Zn alloy bone implants. *J Biomed Mater Res B Appl Biomater.* 2013; 101(2):201–12. https://doi.org/10.1002/jbm.b.32813. PMID: 23115061
4. Chou DT, Hong D, Saha P, Ferrero J, Lee B, Tan Z, et al. In vitro and in vivo corrosion, cytocompatibility and mechanical properties of biodegradable Mg-Y-Ca-Zr alloys as implant materials. *Acta Biomater*. 2013; 9(10):8518–33. https://doi.org/10.1016/j.actbio.2013.06.025. PMID: 23811218
5. Kabir H, Munir K, Wen C, Li Y. Recent research and progress of biodegradable zinc alloys and composites for biomedical applications: Biomechanical and biocorrosion perspectives. *Bioact Mater*. 2020; 6(3):836–879. https://doi.org/10.1016/j.bioactmat.2020.09.013. PMID: 330249903
6. Klauser H. Internal fixation of three-dimensional distal metatarsal I osteotomies in the treatment of hallux valgus deformities using biodegradable magnesium screws in comparison to titanium screws. *Foot Ankle Surg*. 2019; 25(3):398–405. https://doi.org/10.1016/j.fas.2018.02.005. PMID: 30321972
7. Könneker S, Krockenberger K, Pieh C, von Falck C, Brandewiede B, Vogt PM, et al. Comparison of SCAphoid fracture osteosynthesis by MAGnesium-based headless Herbert screws with titanium Herbert screws: protocol for the randomized controlled SCAMAG clinical trial. *BMC Musculoskelet Disord*. 2019; 20:357. https://doi.org/10.1186/s12891-019-2723-9
8. Li G, Yang H, Zheng Y, Chen XH, Yang JA, Zhu D, et al. Challenges in the use of zinc and its alloys as biodegradable metals: Perspective from biomechanical compatibility. *Acta Biomater*. 2019; 97:23–45. https://doi.org/10.1016/j.actbio.2019.07.038. PMID: 31349057
9. Lindtner RA, Castellani C, Tangl S, Zanoni G, Hausbrandt P, Tschegg EK, et al. Comparative biomechanical and radiological characterization of osseointegration of a biodegradable magnesium alloy pin and a copolymeric control for osteosynthesis. *J Mech Behav Biomed Mater.* 2013; 28:232–43. https://doi.org/10.1016/j.jmbbm.2013.08.008. PMID: 24001403
10. Riaz U, Shabib I, Haider W. The current trends of Mg alloys in biomedical applications – A review. *J Biomed Mater Res B Appl Biomater.* 2019; 107(6):1970–1996. https://doi.org/10.1002/jbm.b.34290. PMID: 30536973
11. Song MH, Yoo WJ, Cho TJ, Park YK, Lee WJ, Choi IH. In vivo response of growth plate to biodegradable Mg-Ca-Zn alloys depending on the surface modification. *Int J Mol Sci.* 2019; 20(15):3761. https://doi.org/10.3390/ijms20153761. PMID: 31374825
12. Stürznickel J, Delsmann MM, Jungesblut OD, Stücker R, Knorr C, Rolvien T, et al. Safety and performance of biodegradable magnesium-based implants in children and adolescents. *Injury*. 2021; 52(8):2265–2271. https://doi.org/10.1016/j.injury.2021.03.037
13. Yang H, Jia B, Zhang Z, Qu X, Li G, Lin W, et al. Alloying design of biodegradable zinc as promising bone implants for load-bearing applications. *Nat Commun.* 2020; 11(1):401. https://doi.org/10.1038/s41467-019-14153-7. PMID: 31964879
14. Yu K, Dai Y, Luo Z, Long H, Zeng M, Li Z, et al. In vitro and in vivo evaluation of novel biodegradable Mg-Ag-Y alloys for use as resorbable bone fixation implant. *J Biomed Mater Res A.* 2018; 106(7):2059–2069. https://doi.org/10.1002/jbm.a.36397. PMID: 29569817



**Information about the authors:**

**Denis V. Davydov** — MD, ScD, docent, Head of the Main Military Clinical Hospital named after academician N.N. Burdenko Russian Defense Ministry, Moscow, Russia.

**Artur A. Kerimov** — MD, PhD, Head of the Center of Traumatology and Orthopedics, Main Military Clinical Hospital named after academician N.N. Burdenko Russian Defense Ministry, Moscow, Russia.

**Igor V. Khominets** — MD, PhD, Head of the operational department, Main Military Clinical Hospital named after academician N.N. Burdenko Russian Defense Ministry, Moscow, Russia.

**Dmitry A. Grechukhin** — MD, orthopedic traumatologist, Main Military Clinical Hospital named after academician N.N. Burdenko Russian Defense Ministry, Moscow, Russia — **responsible for contacts**, **dr.grechukhin@gmail.com**, ORCID ID: 0000-0001-7163-7744



*The authors declare no conflicts of interest.*
*The study was not sponsored.*
*Received 13.09.2022*




# Application of regression analysis for differential diagnosis of essential arterial hypertension and neurocirculatory asthenia of the hypertensive type


UDK 616.12-008.1-072.7
DOI: 10.53652/2782-1730-2022-3-3-20-29



**Datsko A.V.[2], Orlov F.A.[1,2,3], Petrova O.N.[2], Dorokhin S.I.[2]**

[1] *Main Military Clinical Hospital named after academician N.N. Burdenko Russian Defense Ministry, Moscow, Russia*
[2] *FGKU «Main center of military medical expertise» of the Ministry of defense of the Russian Federation, Moscow, Russia*
[3] *FGBOU DPO RMANPO of the Ministry of health of Russia, Moscow, Russia*



**Abstract.** In the practice of a military doctor, it is often necessary to make a differential diagnosis between neurocirculatory asthenia (NCA) of the hypertensive type and hypertensive disease (HD) stage I among young and middle-aged military personnel. Both hypertensive NCA and stage I HD patients under examination had autonomic disturbances of varying severity. In patients with NCA of the hypertensive type, the frequency and severity of the autonomic disturbances was higher. It is often not possible to make an accurate differential diagnosis of two diseases based on data from a standard clinical examination and basic laboratory and instrumental investigation methods. By constructing prediction equations for a particular patient with a probability of more than 96.1%, it is possible to calculate the acceptability of relating him to a certain diagnosis.



**Keywords:** arterial hypertension, neurocirculatory asthenia, autonomic nervous system, prognosis of diagnosis.


**Introduction.** According to data from the Center for Military Medical Expertise, in recent years, circulatory diseases have been one of the leading causes of discharge among officers and ensigns (in 2018 the proportion was 26.1% among all classes of diseases). At the same time, there is a decrease in the average age of this category of military personnel recognized as restricted and unfit for military service due to cardiovascular diseases (in 2017 — 41.5 years, in 2014 — 41 years, in 2013 — 49 years, in 2012 — 46.6 years) [1, 2]. At the same time, the discharge rate due to diseases associated with high arterial pressure (AP) remains high, reaching rates ranging from 8.0 to 17.8% in 2012-2017. Over the past 10 years, there has been a 5.3-fold increase in the discharge rate of contract servicemen with hypertension (HD) (from 1.4 ppm in 1999 to 7.9 ppm in 2009), and in conscript servicemen the rate has been 3 to 5% over the past 3 years. Among young and middle-aged servicemen, according to the classification of the World Health Organization (WHO), a differential diagnosis between neurocirculatory asthenia (NCA) of the hypertensive type and Stage I HD often has to be made in the practice of the military doctor [3].

The term "neurocirculatory dystonia" (NCD) proposed and substantiated by N.N. Savitsky (1952), who based this definition on the pathogenetic principle,

**Table 1. Differential diagnostic signs of hypertensive neurocirculatory asthenia and hypertensive disease**

| Signs | Hypertensive neurocirculatory asthenia | Hypertensive disease Stage I |
|---|---|---|
| Burdened heredity for arterial hypertension | Absent | Occurs frequently |
| The character of arterial hypertension | Predominant increase in SAP, often asymmetry of AP in different arms | Frequent elevation of DAP, asymmetry is rare |
| Heart rate | Elevated AP usually accompanied by tachycardia | Changes in heart rate not required |
| Duration of AP elevation | Hours, less often days | Few days |
| Response to hypotensive medications | Uncertain | Distinct |
| Response to diuretics | Unclear | Distinct |
| Response AP on exercise testing | Rapid rise in SAP in phase I of the test to maximum values; DAP rises rarely | Along with SAP, there is often a significant increase in DAP |
| Complaints accompanying the AP increase | Multiple, extremely varied | Usually absent, may be cerebral |

focusing on the mechanisms of disease development, manifested by the disruption of the tone of the central nervous system, which regulates and coordinates the activity of individual parts of the cardiovascular system (CVS), was widely adopted in clinical practice [4, 5, 6, 7, 8].

Thus, hypertensive NCA can be defined as a polyetiological functional disease of the cardiovascular system, which is based on neuroendocrine regulation disorders, manifested by numerous cardiovascular, respiratory and autonomic disorders, asthenization, poor stress and exercise tolerance, characterized by benign course and good prognosis, not leading to cardiomegaly, heart failure and life-threatening heart rhythm disturbances [9, 10, 11].

The autonomic nervous system (ANS), abnormalities of which are caused by NCA syndrome, consists of two departments — parasympathetic and sympathetic. Neurocirculatory asthenia of hypertensive type occurs when in most cases there are disorders on the sympathetic part of the ANS [12, 13, 14].

It is often not easy to diagnose hypertensive NCA. For this purpose the parameters of daily AP monitoring, characteristics of systolic and diastolic AP measurements in dynamics, as well as under physical load are studied. Clinical and instrumental examinations are performed: sonography, obligatory ECG, blood and urine tests. Neurocirculatory dystonia is often to be differentiated from HD, mainly with its early stages. The difficulty of diagnosis is determined by a great similarity of symptoms of NCD and the initial stages of HD, as well as by the fact that both conditions mainly have a hyperdynamic type of circulation. Probably, anamnestic data and prospective observation are of maximal importance in differential diagnosis of NCD and stage I HD. The most important is the indication of unstable AP elevation in NCD and predominance of such elevation in the clinical picture in patients with HD [15, 16].

Hypertensive disease (as defined by the Russian Society of Cardiology in 2010) is a chronic disease, the main manifestation of which is a syndrome of increased AP not associated with the presence of pathological processes, in which increased AP is due to known causes (symptomatic arterial hypertension) [17, 18].

When making an expert decision, it is necessary to proceed from the fact that the diagnosis of hypertension is essentially clinical and anamnestic (at least 6 months of documented anamnesis).

According to a number of studies, even in stage I HD there are often initial manifestations of pathological changes in vessels without signs of target organ lesions [17, 18], whereas there are none in NCA. The characteristic differences in their course and body indices allow to differentiate between NCA and HD and to establish a correct diagnosis. In contrast to HD, in hypertensive NCA there is transient or labile arterial hypertension (AH), no elevated diastolic arterial pressure (DAP), changes in fundus vessels, proteinuria, clinical and instrumental signs of left ventricular (LV) cardiac hypertrophy.

In contrast to hypertensive type NCA, HD is also characterized by:

- taking sedatives has no effect on AP levels;
- blood pressure rises regardless of the situation and time of day, it may rise at night and immediately after waking up;
- AP rarely stabilizes without hypotensive medication;
- Not only does the systolic arterial blood pressure (SAP) rise, but also the DAP.

V.I. Makolkin and S.A. Abbakumov provide differential signs of NCA and stage I HD, presented in Table 1 [19, 20, 21].

In expert work, it is possible to use additional methods to examine the autonomic tone that do not require special analyses and/or equipment. At the same



**Table 2. Scheme of a formalized medical history**

| № | Signs |
|---|---|
| | **Anamnesis** |
| 1. | Age, years |
| 2. | Duration of AH (0 — up to 5 years, 1 — from 5 to 10 years) |
| 3. | Burdened heredity (0 — no, 1 — yes) |
| 4. | Overweight (0 — no, 1 — yes) |
| 5. | Smoking (0 — no, 1 — yes) |
| 6. | Alcohol abuse (0 — no, 1 — yes) |
| 7. | Regularity of administration of hypotensive therapy (0 — episodically, 1 — course treatment) |
| | **Instrumental examination data** |
| | ECG |
| 8. | ECG PQ, s |
| 9. | ECG QRS, s |
| 10. | ECG QT, s |
| 11. | Presence of heart rhythm disorders on ECG (0 — not present, 1 — present) |
| | 24-hour AP monitoring |
| 12. | Mean SAP, mmHg |
| 13. | Mean DAP, mmHg |
| 14. | The limits of fluctuations of average hemodynamic AP, mmHg. |
| 15. | Mean hemodynamic AP, mmHg. |
| 16. | 24-hour AP Index, % |
| | ECG holter monitoring |
| 17. | Average heart rate (HR) during ECG holter monitoring |
| 18. | SVE (0 — absent, 1 — present) |
| 19. | VE (0 — absent, 1 — present) |
| 20. | Average number of supraventricular extrasystoles |
| 21. | Average number of ventricular extrasystoles |
| | Echocardiography |
| 22. | End diastolic size, cm |
| 23. | End systolic size, cm |
| 24. | Diastolic volume, ml |
| 25. | Systolic volume, ml |
| 26. | Stroke volume, ml |
| 27. | Minute volume, l |
| 28. | Ejection fraction, % |
| 29. | LV myocardial mass, g |
| 30. | Diastolic thickness of interventricular septum, cm |
| 31. | Diastolic thickness of LV posterior wall, cm |
| 32. | Left atrial size, cm |
| 33. | Left ventricular myocardial mass index (LV-MMI) |
| 34. | Relative thickness of left ventricular wall (RTLVW) |
| | Veloergometry |
| 35. | Exercise power, W |
| 36. | SAP at the peak of the workload, mmHg |
| 37. | DAP at the peak of the workload, mmHg |
| 38. | HR at the peak of the workload |
| 39. | Myocardial ischemia (MI) (0 — absent, 1 — present) |
| | Biochemical tests |
| 40. | Creatinine, μmol/l |
| 41. | Potassium, mmol/l |
| 42. | Sodium, mmol/l |
| 43. | Total cholesterol, mmol/l |
| 44. | Triglycerides, mmol/l |
| 45. | High density lipoproteins (βlipoproteins), mmol/l |
| 46. | Low-density lipoproteins (pre-βlipoproteins), mmol/l |
| 47. | Very low-density lipoproteins (βlipoproteins), mmol/l |
| | Hormonal examination |
| 48. | Angiotensin I, ng/ml/h |
| 49. | Aldosterone, ng/dL |
| 50. | Cortisol, μg/dL |
| 51. | Thyroid hormone, μIU/ml |
| 52. | Thyiodothyronine, ng/dL |
| 53. | Thyroxine, μg/dL |
| 54. | Adrenocorticotropic hormone, pg/ml |

**Table 3. Characteristics of examined patients with neurocirculatory asthenia of hypertensive type and stage I hypotensive disease**

| Indicices | Neurocirculatory asthenia of hypertensive type | Stage I hypotensive disease |
|---|---|---|
| Number of people examined, n | 20 | 21 |
| Age, years: | | |
| – 18–30; | 16 (80) | 4 (20) |
| – 30–45 | 12 (57,1) | 9 (42,9) |
| Mean age | 21,9±9,5 | 29,4±11,9 |
| Mean duration of AH, years | 1,2±2,3 | 3,2±3,1* |

*p<0.05 when comparing patients with stage I HD and hypertensive NCA. Note. Hereinafter the figures in brackets are the percentage of patients

**Table 4. Four types of diurnal curves depending on the value of the diurnal index**

| The pattern of of nocturnal AP decrease | Type | Percent of nocturnal AP decrease |
|---|---|---|
| Normal | Dipper | 10–20 |
| Insufficient | Non-dipper | 0–10 |
| Nocturnal hypertension | Night-peaker | less 0 |
| Excessive | Over-dipper | more 20 |

time, detection of increased tone of sympathetic nervous system on the basis of several techniques in the presence of basic diagnostic signs predisposes the clinician in favor of NCA diagnosis [22, 3].

**Material and Methods.** The present work is based on the results of a complex clinical-laboratory, hormonal and instrumental examination of 41 men (all men) aged 18–26 years, who were under inpatient examination and treatment in the cardiology department of Main military clinical hospital named after academician N. N. Burdenko from 2015 to 2019. Of them, 21 patients were diagnosed with stage I HD, and 20 patients were diagnosed with hypertensive NCA.

When distributing the material, we followed the classification of HD adopted in the Russian Federation. Verification of the diagnosis and exclusion of symptomatic AH was performed on the basis of a two-stage examination system developed and recommended by the A. L. Myasnikov Institute of Clinical Cardiology of the Scientific Medical Research Center of Cardiology of the Russian Academy of Medical Sciences.

There were no additional criteria for inclusion of patients in the study. At the same time, persons older than 45 years, with clinical signs of CHD, symptomatic arterial hypertension, other concomitant diseases of cardiovascular system and internal organs were not included in the study.

The patient examination program contained clinical indices and laboratory instrumental methods presented in the formalized medical history (MH) (Table 2), which allowed to create a computer database later on.

All obtained results were summarized in a formalized MH in which qualitative features were presented in quantitative gradations and quantitative features were given in their absolute values. The first seven features were anamnestic data, including age, duration of AH, and risk factors for the disease.

After clinical, laboratory and instrumental examinations, the main results of which were included into the formalized MH, we applied mathematical methods of the ANS state examination in the form of a regression analysis for a more detailed assessment of the autonomic status [6].

Regression is the dependence of the mean value of one random variable on some other (or several random variables), while regression analysis is a branch of mathematical statistics that incorporates applied methods for studying regression dependencies [24]. When performing a regression analysis, it is important to correctly choose the type and degree of complexity of the regression model. The classical way is to take into consideration biological, physical and other assumptions, and the quality of the obtained model is assessed by the value of residual deviations. It is possible to test the hypothesis of linearity by





residual deviations – the nonlinearity index is calculated and the reliability of its difference from zero is checked by Fisher's criterion.

As a result of regression analysis, the following equation was obtained:

$$Y = K + A_1 X_1 + A_i X_i + \dots ,$$

where: Y — predicted trait; K — constant term of the equation; A — weighting factor for the trait included in the equation; X — quantitative value of the given trait. The obtained regression equations allow to determine a specific value of the predicted attribute (in this case, the number of ventricular extrasystoles per day) by using the data of clinical and instrumental examination of a particular patient. Discriminant equations can give an answer about the presence or absence of the trait by the value of the constant (to predict the absence or presence of MI during holter ECG monitoring).

Traits (X) included in the prediction equations with a positive sign have a direct dependence on the value of the predicted trait: for example, the greater the LV myocardial mass or age in patients with hypertension, the greater the predicted number of ventricular extrasystoles during ECG monitoring. The signs included in the equation with a negative sign have an inverse relationship: for example, the lower the systolic volume and ejection fraction in patients with AH and abdominal obesity, the higher the predicted number of ventricular arrhythmias in them.

The residual dispersion reflects the probability of predicting a particular trait in percent, and the degree of difference between the obtained dependence and the linear equation can be determined by the formula:

$$y = \sqrt{1 - R^2} .$$

Results were processed on a personal computer using Statistica 6.0 software. The Kolmogorov-Smirnov and Shapiro-Wilk criteria were used to check the distribution for normality. For normal distribution, quantitative signs were presented as mean ± standard deviation (M±a).

Relative values were compared using the $\chi 2$ criterion. In all cases of hypothesis testing, the differences were considered statistically significant at $p<0.05$ [25, 26, 27, 28].

General characteristics of the examined patients with HD and NCA are shown in Table 3.

**Results and discussion.** It can be seen from the table that the mean age of stage I HD patients was 29,4±11,9years, in hypertensive type NCA — 21,9±9,5 years. NCA patients were younger, but the groups were comparable according to the main indices. In both groups, individuals in the age range from 18 to 30 years prevailed. At the same time, the mean duration of AH in HD patients was significantly longer than in NCA and was 3,2±3,1 and 1,2±2,3 years, respectively. Nine patients with HD had been previously diagnosed with hypertensive NCA.

Excessive body weight, smoking, and alcohol consumption (at least once a week in an amount greater than 150 ml) were observed more frequently in patients with HD than in those with NCA. The factor of hereditary AH in the closest relatives was significantly more frequent in patients with HD compared to NCA — 87.5 and 25%, respectively.

The survey of the patients revealed various subjective disorders in them. The most frequent clinical manifestations in both groups of patients were headaches (mostly mild) — 85 and 95.2%; dizziness — 15 and 52.4%; neurotic disorders — 100 to 61.9%. Headaches in NCA patients were of diverse character, not always associated with an increase in AP, and more often had a migraine-like character. Their aggravation was associated with psycho-emotional tension and changes in meteorological conditions. Group 2 patients had headaches more often in the morning and evening hours, weakened in the middle of the day, were dull, pressing, localized mainly in the occipital area and were associated with AP destabilization. Dizziness was predominantly observed in Group 2 patients and was usually of a short-term nature, and did not significantly affect well-being.

Assessment of the peculiarities of daily AP rhythm is carried out on the basis of the results of daily AP monitoring. This examination is absolutely necessary for expert evaluation of a patient, decision-making on prescription and necessity of correction of antihypertensive therapy. It is of great interest to assess the differences between the mean values of daytime and night-time AP, i.e., the expressiveness of AP biphasic rhythm during a day. It is generally accepted, that a healthy person should have 10–20% decrease of SAP and DAP at night. The simplest and widely used method in clinical practice to assess the diurnal rhythm of AP is the calculation of the degree of night-time AP decrease — Diurnal Index (DI) (Table 4).

The diurnal index is calculated according to the following formula:

$$DI=100\%\times(APd-APn) / APd,$$

Where: APd — is the average AP during the waking period; APn — is the average AP during the sleeping period.

Table 5 shows the main AP indicices in the examined patients. We can see that the mean values of both SAP and DAP were elevated in both groups.

**Table 5. Blood pressure indicices in the examined patients**

| № | Indicices | Neurocirculatory asthenia of the hypertensive type, n=20 | Stage I hypotensive disease, n=21 |
|---|---|---|---|
| 1. | Variation limits of SAP fluctuations, mmHg. | 120–180 | 125–180 |
| 2. | Variation limits of DAP fluctuations, mmHg. | 70–90 | 70–95 |
| 3. | Mean SAP, mmHg. | 161,2±12,2 | 116,5±2,2 |
| 4. | Mean DAP, mmHg. | 79,0±12,6 | 78,0±13,1 |
| 5. | Variation limits of mean hemodynamic AP, mmHg. | 90–150 | 89–149 |
| 6. | Variation limits of mean hemodynamic AP, mmHg. | 117,0±11,6 | 118,0±15,6 |
| 7. | Diurnal index of AP, mean | 13% | 9,8%* |
| *p<0.05 when comparing patients with HD stage I and hypertensive NCA. | | | |

**Table 6. Indices needed to predict probable diagnosis in patients with arterial hypertension (5% residual dispersion)**

| № | Trait (Xi), coding | Weighting Coefficient (Ai) | F-criterion | Rank of the trait |
|---|---|---|---|---|
| 1. | Body mass index (BMI) | +0,019 | 13,6 | 1 |
| 2. | Burdened heredity for AH | -0,024 | 8,2 | 3 |
| 3. | Angiotensin I, ng/ml/h | +0,094 | 8,7 | 2 |
| 4. | QRS complex width, ms | -3,38 | 7,6 | 4 |
| 5. | Creatinine, mmol/l | -0,0017 | 5,9 | 6 |
| 6. | Cholesterol, mmol/l | +0,043 | 5,7 | 7 |
| 7. | Diastolic thickness of LV posterior wall, cm | +0,0082 | 2,9 | 11 |
| 8. | Aldosterone, ng/dL | +0,013 | 3,2 | 10 |
| 9. | LV end diastolic size, cm | -0,134 | 4,8 | 8 |
| 10. | Age, years, лет | +0,122 | 4,7 | 9 |
| 11. | SAP, mmHg | +0,109 | 6,45 | 5 |
| | Constant (A0) | 0,408 | | |
| | R1 | 0,1664 | | |
| | R2 | | | |



The SAP in NCA patients ranged from 120 to 180 mmHg, and in stage I HD — from 125 to 180 mmHg, and DAP — from 70 to 90 and 70 to 95 mmHg, respectively. Mean DI was 13% in NCA and 9.8% in HD.

When analyzing the average indices of the main instrumental methods of cardiovascular examination in the studied subjects, there were no significant differences in patients with hypertensive type NCA and stage I HD. In addition to 24-hour AP monitoring all patients underwent ECG, echocardiography, veloergometry, 24-hour holter ECG monitoring. This fact gives relevance to the issues of differential diagnostics of these diseases. Only an increase in the average number of ventricular extrasystoles during a day in patients with HD was revealed, which did not exceed the normative value.

Thus, it is not possible to make a differential diagnosis of the two diseases on the basis of basic laboratory and instrumental methods of examination. For this purpose, we included the methods of mathematical evaluation of the ANS state into the study.

We also studied the possibility of predicting the assignment of a particular patient to one or another group of probable hypertensive NCA or HD diagnosis by substituting the data of his clinical, biochemical, and instrumental examination into the prediction equation obtained by regression analysis (Table 6).

From the above equation we can see that the most significant indices (guided by the sign rank) necessary for predicting the diagnosis in a patient with AH are BMI, angiotensin I blood level, heredity for AH, and creatinine level.

When calculating the probability of the development of HD using clinical and instrumental examination parameters of a patient with AH, if the following condition is met

$$G(X)=\sum_{i=1}^{n} XiWi \leq 464{,}32,$$

then such a patient is prognosed to have hypertensive NCA.

If these conditions are not met, i.e.

$$G(X)>464{,}32,$$

then the patient is more likely to have HD. Of the 21 patients with a previously established diagnosis of Stage I HD, 18 (85.7%) patients were correctly classified when their values were included in the prognostic equation, and 3 (14.3%) patients were assigned to the hypertensive type of NCA. Thus, the overall prediction accuracy in this case was 96.1%.

We can also assume the great importance of the indices included in the equation of diagnosis prediction in further development of cardiovascular complications in AH patients and the necessity of their monitoring in the follow-up of a patient with AH.

**Conclusions.** In the examined patients with both hypertensive NCA and stage I HD the autonomic disturbances were of varying severity. In patients with hypertensive type NCA the frequency and severity of the latter were greater.

To make an accurate differential diagnosis of the two diseases based only on the data of standard clinical examination, basic laboratory and instrumental methods of investigation is often not possible due to the absence of significant differences in these indices.

By constructing prediction equations for a particular patient with a probability of more than 96.1%, it is possible to calculate the admissibility of assigning him to one or another diagnosis.

The use of regression analysis will allow the physician to accurately make a diagnosis, while the indices included in the prediction equation may indicate an initial, not yet identified target organs lesion, which cannot be detected at the current stage of diagnostic equipment development.

**References**

1. Bulavin VV, Chapluk AL, Kalmanov AS, Datsko AV, Denisova MP. The role of risk-factors in formation of arterial hypertension in teenagers, prospective conscripts and conscripts. *Russian Military Medical Journal.* 2015; 336(11):56–60. (In Russ.). https://doi.org/10.17816/RMMJ74041
2. Shklovskii BL, Prokhorchik AA. Military-medical examination for cardiovascular diseases in the central military clinical hospital. *Russian Military Medical Journal*. 2018; 339(6):9–17. (In Russ.)]. https://doi.org/10.17816/RMMJ72945
3. Avtandilov AG. *Arterial'naya gipertenziya u podrostkov muzhskogo pola.* Moscow: Russian Medical Academy of Continuous Professional Education; 1997. 285 p. (In Russ.)].
4. Grinshtein AM, Popova NA. *Vegetativnye sindromy*. Moscow: Meditsina; 1971. 308 p. (In Russ.).
5. Drobotya NV. Gemodinamicheskiye reaktsii na vneshniye vozdeystviya u zdorovykh lyudey i u bolnykh neyrotsirculyatornoy distoniey. In: *Eksperimentalnaya i klinicheskaya fiziologiyakrovoobrashcheniya.* Cheboksary; 1993. p. 85–89. (In Russ.).
6. Makolkin VI, Abakumov SA. *Neyrotsirculatornaya distoniya v therapevticheskoy praktike.* Moscow: Meditsina; 1985. 192 p. (In Russ.).
7. Pokalev GM. *Neyrotsirkulatornaya distoniya.* Nizhniy Novgorod: Publishing house of the NGMI; 1994. 300 p. (In Russ.).
8. Tzivoni D, Stern Z, Keren A, Stern S. Electrocardiographic characteristics of neurocirculatory asthenia during everyday activities. *Br Heart J.* 1980; 44(4):426–32. https://doi.org/10.1136/hrt.44.4.426
9. Chazova IE, Danilov NM, Litvin AYu. *Refracternaya arterialnaya hipertoniya: Monografiya.* Moscow: Atmosfera; 2014. 256 p. (In Russ.).
10. Hynynen E, Konttinen N, Kinnunen U, Kyröläinen H, Rusko H. The incidence of stress symptoms and heart rate variability during sleep and orthostatic test. *Eur J Appl Physiol.* 2011; 111(5):733–41. https://doi.org/10.1007/s00421-010-1698-x

11. Lee H, Kim HA. Orthostatic hypertension: An underestimated cause of orthostatic intolerance. *Clin Neurophysiol.* 2016; 127(4):2102–7. https://doi.org/10.1016/j. clinph. 2015.12.017
12. Veyn AM, Voznesenskaya TG, Vorobyova OV. *Vegetativnye rasstroystva: Klinika, lecheniye, diagnostika.* A.M. Veyn, editor. Moscow: Meditsinskoe informatsionnoye agentstvo; 2003. 752 p. (In Russ.).
13. Anshelevich YuV, Gurvich T.R. Autonomic regulation of the heart in the circulatory dystonia. *Clinical Medicine.* 1987;65(5):61–64. (In Russ.).
14. Wayne AM, Solov[illegible]eva AD, Kolosova OA. *Vegetososudistaya distoniya*. Moscow: Meditsina; 1981. 318 p. (In Russ.).
15. Sklyannaya EV. The role of orthostatic test in prognosis of arterial hypertension development in young adults. *Clinician*. 2018; 12(2):16–21. (In Russ.). https://doi.org/10.17650/1818-8338-2018-12-2-16-21
16. Sorokina TA. *Neyrotsirkulatornaya distoniya.* Riga: Zinatne; 1979. 176 p. (In Russ.).
17. Guidelines for the treatment of arterial hypertension of the European Society for Hypertension (ESH) and the European Society of Cardiology( ESC), November 2017.
18. Mancia D, Fagard R, Narkiewicz K, Redón J, Zanchetti A, Böhm M, et al. 2013 ESH/ESC Guidelines for the management of arterial hypertension: the Task Force for the management of arterial hypertension of the European Society of Hypertension (ESH) and of the European Society of Cardiology (ESC). *J Hypertens.* 2013; 31(7):1281–357. https://doi.org/10.1097/01.hjh.0000431740.32696.cc. PMID: 23817082
19. Savitskiy NN. O nomenklature i klassifikatsii zabolevaniy serdechno-sosudistoy sistemy nevrogennoy prirody. *Clinical Medicine.* 1964; 42(3):20. (In Russ.).
20. Snezhitskiy VA. Methodicheskiye aspekty provedeniya ortostaticheskikh prob dlya otsenki sostoyaniya vegetativnoy nervnoy sistemy i funktsii sinusovogo uzla. *Journal of the Grodno State Medical University.* 2006; (1):3–6. (In Russ.).
21. Solovyova SV, Tsertsek TN, Bakieva EM, Trusevich NV, Solovyov VS. Active orthostatic responses in healthy persons and AH and COPD patients in the Surgut-city. *Tyumen State University Herald.* 2014; (6):132–40. (In Russ.).
22. Almazov VA, Shlyakhto EV, Sokolova L.A. *Pogranichnaya arterial'naya gipertenziya*. Saint-Petersburg: Gippokrat; 1992. 192 p. (In Russ.)].
23. Resolution of the Government of the Russian Federation No. 565 of July 4, 2013 "On Approval of the Regulations on Military Medical Expertise". (In Russ.)].
24. Bailey NTJ. *The mathematical approach to biology and medicine /* Translated from English by Kovalenko EG. Moscow: Mir; 1970. 326 p. (In Russ.).
25. Adler YuP, Markova EV, Granovsky YuV. *Planirovaniye eksperimenta pri poiske optimal'nykh usloviy*. Moscow: Nauka; 1971. (In Russ.).
26. Kluzhev VM. Application of mathematical modeling methods in clinical practice. *Russian Military Medical Journal.* 1997;(5):41–44. (In Russ.).
27. Lasted LB. *Introduction to medical decision making.* Bykhovskiy ML, editor; translated from English by Bykhovskaya IM. Moscow: Mir; 1991. 282 p. (In Russ.).
28. Lisenkov AN. *Mathematicheskiye methody planirovaniya mnogofaktornykh medico-biologicheskikh eksperimentov*. Moscow: Meditsina; 1979. 343 p. (In Russ.).

**Information about the authors:**

**Andrej V. Datsko** — Colonel of Medical Service, Chief Military Medical Expert of the Defense Ministry, Chief of the FGKU «Main center of military medical expertise» of the Ministry of defense of the Russian Federation, Moscow, Russia.

**Filipp A. Orlov** — MD, ScD, Associate Professor, Honored Doctor of the Russian Federation, Head of Therapeutic (Advisory) Department, Main Military Clinical Hospital named after academician N.N. Burdenko Russian Defense Ministry, Moscow, Russia — **responsible for contacts**, **esculap1@rambler.ru**, ORCID: 0000-0002-7081-9623

**Ol'ga N. Petrova** — Lieutenant Colonel of the Medical Service, Head of the Department of Examination of Military Personnel and Special expertise, FGKU «Main center of military medical expertise» of the Ministry of defense of the Russian Federation, Moscow, Russia.

**Stanislav I. Dorohin** — Captain of Medical Service, Head of Department of Examination of Military Personnel and Special Expertise, FGKU «Main center of military medical expertise» of the Ministry of defense of the Russian Federation, Moscow, Russia.

*The authors declare no conflicts of interest.*
*The study was not sponsored.*
*Received 30.05.2022*



# Nomogram M validity assessment for predicting multiple organ failure and acute kidney injury after elective cardiac surgery with cardiopulmonary bypass

UDK 616.61-008.6
DOI: 10.53652/2782-1730-2022-3-3-30-37

**Berikashvili L.B.[1, 2], Smirnova A.V.[3], Laricheva E.A.[3], Gracheva N.D.[1], Kadantseva K.K.[1, 4], Yadgarov M.Y.[1], Grechko A.V.[5]**

[1] *Department of clinical trials of V.A. Negovsky Research Institute of General Reanimatology, Federal Research and Clinical Center of Intensive Care Medicine and Rehabilitology, Moscow, Russia*
[2] *Intensive care department M.F. Vladimirsky Moscow Regional Research Clinical Institute, Moscow, Russia*
[3] *First Moscow State Medical University (Sechenov University), Moscow, Russia*
[4] *A. Loginov Moscow Clinical Scientific Center, Moscow, Russia*
[5] *Federal Research and Clinical Center of Intensive Care Medicine and Rehabilitology, Moscow, Russia*

**Abstract.** ***Purpose.*** To evaluate the predictive value of nomogram M for multiple organ failure (MOF) and acute kidney injury (AKI) after elective cardiac surgery with cardiopulmonary bypass.
***Materials and methods.*** This was a retrospective cohort study. The predictive value of nomogram M for multiple organ failure and acute kidney injury after elective cardiac surgery with cardiopulmonary bypass was evaluated using ROC-analysis.
***Results.*** The sample size was 158 patients. The incidence of AKI was 5.7% (9 of 158 patients). The incidence of MOF was 3.8% (6 of 158 patients). AUC nomogram M for AKI was 0.714 [95% CI: 0.555–0.874] (p=0.031); the cut-off value was 12,5 points; the sensitivity was 66.67% and specificity was 82.55%; the odds ratio was 9.46 (95% CI: 2.22–40.30) (p<0.001). AUC nomogram M for MOF was 0.770 [95% CI: 0.594–0.946] (p=0.025); the cut-off value was 12,5 points; the sensitivity was 83.33% and specificity was 82.24%; the odds ratio was 23.15 (95% CI: 2.60–206.20) (p<0.001).
***Conclusion.*** Nomogram M has an acceptable predictive value for multiple organ failure and acute kidney injury after elective cardiac surgery with cardiopulmonary bypass based on the results of the ROC-analysis.

**Keywords:** cardiac surgery, cardiopulmonary bypass, acute kidney injury, multiple organ failure, postoperative complications, prognostic scale.

**Introduction.** Acute kidney injury (AKI) and multiple organ failure syndrome (MOFS) developing after cardiac surgery are serious complications associated with the adverse course of the postoperative period [1, 2]. In particular, both of these outcomes are associated with hospital mortality [3-6] and length of stay in intensive care unit (ICU) [6, 7]. At the same time, for example, the incidence of AKI after cardiac surgeries can reach 30% [8]. Currently, it is known that the main risk factors of this outcome after cardiac surgery are age, chronic kidney diseases, chronic obstructive pulmonary disease (COPD), diabetes mellitus (DM), atherosclerotic damage of peripheral

arteries, chronic heart failure, left ventricular (LV) ejection fraction <35%, use of cardiopulmonary bypass (CPB) during cardiac surgery, the duration of CPB [9]. Due to the fact that these outcomes strongly influence the course of postoperative period, the possibility of distinguishing the risk groups of these outcomes appears to be an extremely important decision-making tool in clinical practice.

Previously, to predict the course of postoperative period after elective cardiac surgery under CPB, a nomogram M was proposed which demonstrated high prognostic ability relative to 30-day mortality [10], good prognostic ability relative to the development of serious adverse cardiac and cerebral events [11] and new postoperative hemodynamically significant arrhythmias [12]. Nomogram M includes 10 parameters for evaluation: age, sex, body mass index, poor mobility, glomerular filtration rate (GFR) class, resting angina, recent antiaggregant use, LV ejection fraction, critical preoperative state and vasoactive inotropic scale value at the moment of admission to ICU from operating room.

This work assessed the prognostic ability of the nomogram M in relation to outcomes such as AKI and MOF syndrome.

**Objective.** To investigate the prognostic ability of the nomogram M in relation to the development of AKI and MOFS during hospitalization after elective cardiac surgery under CPB conditions.

**Material and Methods.** A single-center retrospective cohort study was carried out; it included the study of medical records of cardiac surgery patients who underwent surgical intervention between June 2014 and September 2017.

The inclusion criteria were age over 18 years and elective cardiac surgery under CPB conditions; the exclusion criteria were congenital heart defects. In the present study the following data were collected and statistically analyzed: age, sex, height, body weight, GFR, preoperative creatinine level, chronic dialysis, LV ejection fraction, history of myocardial infarction, resting angina, arterial hypertension, DM, COPD, cirrhosis, stroke history, poor mobility (according to E-CABG [13] and Euroscore 2 criteria [14]), severity of patients' preoperative condition (according to E-CABG [13] and Euroscore 2 criteria [14]), recent antiaggregant use [15], VIS [16] at the time of ICU admission from the operating room.

The primary endpoints chosen were the incidence rates of AKI and MOFS during hospitalization.

The principle of using the nomogram M is described in detail in a previously published paper [11].

An ROC analysis was performed to determine the prognostic ability of the nomogram M in relation to AKI and MOFS during the period of initial hospitalization. A cutoff point was calculated for the nomogram M. This value of the nomogram M served as the rule for dividing

**Table 1. Nomogram M**

| Parameters | Scores |
|---|---|
| VIS at the time of admission to the ICU (score): | |
| <8 | 0 |
| 8–15 | 2 |
| >15 | 4 |
| Critical preoperative condition | 4,5 |
| LV ejection fraction (%): | |
| >50 | 0 |
| 31–50 | 1 |
| 21–30 | 5 |
| ≤20 | 6,5 |
| Resting angina pectoris | 2 |
| Poor mobility | 3 |
| Recent use of antiaggregants | 2 |
| MDRD eGFR (grade): | |
| 1 | 0 |
| 2 | 0 |
| 3a | 1 |
| 3b | 4,5 |
| 4 | 7 |
| 5 | 8 |
| Body mass index (kg/m²): | |
| 15 | 2 |
| 20 | 2,5 |
| 25 | 3 |
| 30 | 4 |
| 35 | 4,5 |
| 40 | 5 |
| 50 | 6,5 |
| Female gender | 0,5 |
| Age (years): | |
| 20 | 2 |
| 30 | 3 |
| 40 | 4 |
| 50 | 5 |
| 60 | 6 |
| 70 | 7 |
| 80 | 8 |

Note: MDRD eGFR — calculated glomerular filtration rate using MDRD formula; VIS — vasoactive inotropic scale.



patients into two groups: group 1 — patients who scored less than the cutoff point, group 2 — patients who scored equal to or greater than the cutoff point.

Normality of distribution was assessed for the collected data. Quantitative results with a normal distribution are presented as mean and standard deviation, while data with a distribution other than normal are presented as median and quartiles (IQR, interquartile range).

Statistical analysis of the data was performed using the software packages IBM SPSS Statistics 25.0 and MedCalc® Statistical Software version 20.008 (MedCalc Software Ltd, Ostend, Belgium). Normality of the distribution was assessed using the Shapiro-Wilk test. The critical p-value was set at 0.05. ROC-analysis was used to assess predictive ability of various parameters, assessing the AUC parameter (area under the ROC-curve) and its 95% confidence interval (CI). The threshold value was chosen based on the optimal sensitivity/specificity ratio according to the results of ROC analysis (Youden's J statistic). Sensitivity, specificity, accuracy, and odds ratio (OR) were calculated for predictors.

**Results.** The medical records of 520 patients were examined as part of the study. The inclusion and exclusion criteria were met in 158 patients. All 158 patients were included in the final analysis (Fig. 1).

The preoperative characteristics of the cohort are presented in Table 2. Comorbidity of patients is shown in Table 3. The types of surgical intervention are presented in Table 4.

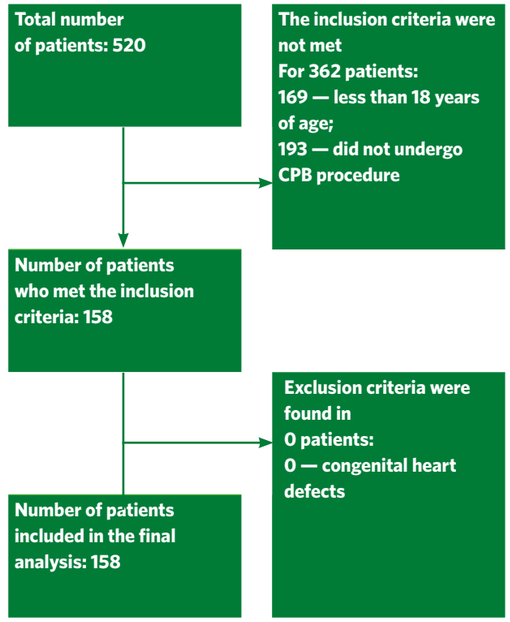


**Fig. 1.** Scheme of inclusion of patients in the study

**Table 2. Preoperative characteristics of the patient cohort**

| Parameters | Value |
|---|---|
| Age (years) | 60,19 ± 7,99 |
| Number of men (person, %) | 124 (78,48%) |
| Body mass index (kg/m2) | 28,52 ± 3,78 |
| Creatinine concentration in plasma (μmol/l) | 94 [86; 105] |
| Glomerular filtration rate (ml/min) | 82,83 [66,19; 95,66] |
| LV ejection fraction (%) | 58,72 ± 10,22 |

**Table 3. Comorbidity of patients**

| Chronic diseases | Number of patients, n (%) |
|---|---|
| Arterial hypertension | 114 (72,2%) |
| Chronic obstructive pulmonary disease | 9 (5,7%) |
| Active endocarditis | 4 (2,5%) |
| Insulin dependent diabetes mellitus | 9 (5,7%) |
| Myocardial infarction within 90 days prior to surgery | 7 (4,4%) |
| Pulmonary arterial hypertension | 23 (14,6%) |
| Atherosclerotic lesion of non-coronary arteries | 32 (20,3%) |
| History of resting angina pectoris | 6 (3,8%) |

**Table 4. Types of surgical interventions**

| Type of surgery | Number of patients (n, %) |
|---|---|
| Coronary artery bypass surgery | 125 (79,12%) |
| Surgery on any one valve | 13 (8,23%) |
| Coronary artery bypass grafting combined with aneurysmectomy | 9 (5,7%) |
| Surgery on any one valve combined with aneurysmectomy | 5 (3,17%) |
| Coronary artery bypass graft combined with surgery on any one valve | 1 (0,63%) |
| Coronary artery bypass graft combined with surgery on one valve and aneurysmectomy | 1 (0,63%) |
| Operation on 2 any valves combined with aneurysmectomy | 2 (1,26%) |
| Operation on any 2 valves combined with coronary artery bypass grafting | 1 (0,63%) |
| Operation on 3 valves combined with aneurysmectomy | 1 (0,63%) |

The median value of the vasoactive inotropic scale at the time of admission to the ICU from the operating room is 1.5 scores [IQR: 0; 5.0]. The median value of the nomogram M is 10.0 points [IQR: 9.0; 11.4].

***Acute kidney injury.*** The incidence of AKI during hospitalization was 5.7% (9 of 158 patients), the AUC nomogram M parameter=0.714 [0.555; 0.874] (p=0.031) (Figure 2), the cutoff point was 12.5 points (sensitivity, 66.67% [95% CI: 29.93%; 92.51%], specificity, 82.55% [95% CI: 75.49%; 88.27%]).

The predictive value of a positive result was 18.75% [95% CI: 11.45%; 29.17%], the predictive value of a negative result was 97.62% [95% CI: 94.20%; 99.04%], and the accuracy of the predictive model was 81.65% [95% CI: 74.72%; 87.35%].

The absolute risk of developing AKI during hospitalization in group 1 (patients scoring less than 12.5) was 2.4% (3 of 126 patients) and in group 2 (patients scoring 12.5 or more) was 18.8% (6 of 32 patients). The odds ratio of group 2 versus group 1 was 9.46 [95% CI: 2.22; 40.30], p<0.001.

***Multiple organ failure syndrome.*** The incidence of MOFS during hospitalization was 3.8% (6 of 158 patients), the $AUC_{nomogram\ M}$ parameter=0.770 [0.594; 0.946] (p=0.025) (Fig. 3), cutoff point was 12.5 points (sensitivity, 83.33% [95% CI: 35.88%; 99.58%], specificity, 82.24% [95% CI: 75.22%; 87.96%]).

The predictive value of a positive result was 15.62% [95% CI: 10.14%; 23.30%], the predictive value of a negative result was 99.21% [95% CI: 95.42%; 99.87%], and the accuracy of the predictive model was 82.28% [95% CI: 75.42%; 87.89%].

The absolute risk of developing MOFS during hospitalization in group 1 (patients scoring less than 12.5) was 0.8% (1 of 126 patients) and in group 2 (patients scoring 12.5 or more) was 15.6% (5 of 32 patients). The odds ratio of group 2 versus group 1 was 23.15 [95% CI: 2.60; 206.20], p<0.001.

**Discussion.** Based on the results of the study, we can conclude that the nomogram M has acceptable prognostic ability regarding the development of AKI ($AUC_{nomogram\ M}$=0.714 [0.555; 0.874], p=0.031) and MOFS ($AUC_{nomogram\ M}$=0.770 [0.594; 0.946], p=0.025) after elective cardiac operations performed under CPB conditions.

It is also worth noting that the cutoff point for both outcomes is 12.5 points, which greatly facilitates the interpretation of the results and the process of predicting outcomes. The odds ratio for AKI relative to this cutoff point is 9.46 [95% CI: 2.22; 40.30] (p<0.001) and for MOFS is 23.15 [95% CI: 2.60; 206.20] (p<0.001). Note that both outcomes have fairly wide 95% CIs. In this case, a more correct approach would be to interpret the results of the study relative to the lower limit of the 95% CI.

Consequently, with a 95% probability, we can state that the chance of developing AKI in patients who scored 12.5 or more on the nomogram M is at least 2.2 times higher, and the chance of developing MOFS is at least 2.6 times higher.

When evaluating the prognostic power of the nomogram M in relation to AKI and MOFS, it was shown that the lower limits of the 95% CI for sensitivity were less than 50%. This result indicates that only a one-sided interpretation of the results is possible based on the nomogram M. This is also supported by the low values of the prognostic significance of positive results for both outcomes: 18.75% [95% CI: 11.45%; 29.17%] for AKI and 15.62% [95% CI: 10.14%; 23.30%] for MOFS.

Thus, the nomogram M does not allow directly to identify high-risk groups for AKI and MOFS after elective cardiac surgeries under CPB conditions.

In contrast, the high specificity of the nomogram M for both outcomes (82.55% for AKI and 82.24% for MOFS), combined with the very high predictive value of a negative result (over 95%), indicates that the nomogram M provides a high probability of identifying a group of low-risk patients for AKI and MOFS after elective cardiac surgery with CPB (patients with a score of less than 12.5). Consequently, nomogram M provides an opportunity to identify the group of patients requiring more careful monitoring in the postoperative period by excluding the group of low-risk patients with AKI and MOFS.



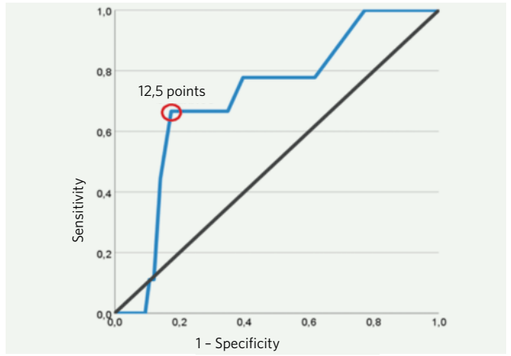


**Fig. 2.** Assessment of the prognostic ability of the nomogram M in relation to the development of acute kidney injury during hospitalization

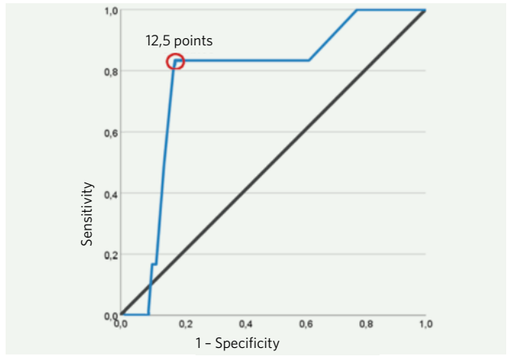


**Fig. 3.** Assessment of the prognostic ability of the nomogram M in relation to the development of multiple organ failure syndrome during hospitalization

***External validity.*** The external validity of the study is high for the group of patients who are scheduled for elective cardiac surgery under CPB. Nevertheless, the results of this category of patients cannot be extrapolated to all types of surgical interventions, which to some extent reduces the external validity of the study. However, the absence of direct confirmations of the validity of the nomogram M in relation to other categories of patients is a reason for further evaluation of the prognostic ability of this model.

**The prognostic ability of Nomogram M regarding the development of acute kidney injury and multiple organ failure syndrome during hospitalization after elective cardiac surgeries performed using cardiopulmonary bypass, based on ROC-analysis, is characterized as satisfactory**

***Limitations.*** Three limitations were identified for this study:

- the study is single-center and retrospective, which reduces the significance of the results;
- patients (79.12%) underwent coronary artery bypass grafting, which reduces the accuracy of extrapolation of the results to other types of cardiac interventions;
- the nomogram M demonstrated only one-sided interpretation of the results related to the allocation of risk groups regarding the development of AKI and MOFS after elective cardiac surgeries in the AC setting.

**Conclusion.** The prognostic ability of Nomogram M regarding the development of acute kidney injury and multiple organ failure syndrome during hospitalization after elective cardiac surgeries performed using cardiopulmonary bypass, based on ROC-analysis, is characterized as satisfactory.

**References**

1. Chew STH, Hwang NC. Acute Kidney Injury After Cardiac Surgery: A Narrative Review of the Literature. *J Cardiothorac Vasc Anesth*. 2019 Apr; 33(4):1122–1138. https://doi.org/10.1053/j.jvca.2018.08.003. PMID: 30228051
2. Babayev MA, Yeremenko AA, Vinnitsky LI, Bunyatyan KA. Causes of Multiple Organ Dysfunction During Cardiosurgical Operations under Extracorporeal Circulation. *General Reanimatology*. 2010; 6(3):76–81. (In Russ.). https://doi.org/10.15360/1813-9779-2010-3-76
3. Asim M, Amin F, El-Menyar A. Multiple organ dysfunction syndrome: Contemporary insights on the clinicopathological spectrum. *Qatar Med J*. 2020 Sep 22; 2020(1):22. https://doi.org/10.5339/qmj.2020.22. PMID: 33628712
4. Soo A, Zuege DJ, Fick GH, Niven DJ, Berthiaume LR, Stelfox HT, et al. Describing organ dysfunction in the intensive care unit: a cohort study of 20,000 patients. *Crit Care*. 2019 May 23; 23(1):186. https://doi.org/10.1186/s13054-019-2459-9. PMID: 31122276

5. Wang HE, Muntner P, Chertow GM, Warnock DG. Acute kidney injury and mortality in hospitalized patients. *Am J Nephrol*. 2012; 35(4):349–55. https://doi.org/10.1159/000337487. PMID: 22473149
6. Bedford M, Stevens PE, Wheeler TW, Farmer CK. What is the real impact of acute kidney injury? *BMC Nephrol*. 2014 Jun 21; 15:95. https://doi.org/10.1186/1471-2369-15-95. PMID: 24952580
7. Barie PS, Hydo LJ. Influence of multiple organ dysfunction syndrome on duration of critical illness and hospitalization. *Arch Surg*. 1996 Dec; 131(12):1318–23. https://doi.org/10.1001/archsurg.1996.01430240072010. PMID: 8956774
8. Hoste EA, Cruz DN, Davenport A, Mehta RL, Piccinni P, Tetta C, et al. The epidemiology of cardiac surgery-associated acute kidney injury. *Int J Artif Organs*. 2008 Feb; 31(2):158–65. https://doi.org/10.1177/039139880803100209. PMID: 18311732
9. Wang Y, Bellomo R. Cardiac surgery-associated acute kidney injury: risk factors, pathophysiology and treatment. *Nat Rev Nephrol*. 2017 Nov; 13(11):697–711. https://doi.org/10.1038/nrneph.2017.119. PMID: 28869251
10. Berikashvili LB, Kuzovlev AN, Yadgarov MYa, Ovezov AM, Ryabova EV, Kadantseva KK, et al. Influence of pre- and intraoperative factors on hospital mortality after elective cardiac surgery with cardiopulmonary bypass. A retrospective study. *Annals of Critical Care*. 2021; 2:128–135. (In Russ.). https://doi.org/10.21320/1818-474X-2021-2-128-135
11. Berikashvili LB, Kuzovlev AN, Yadgarov MYa, Kadantseva KK, Ozhiganova EA, Likhvantsev VV. Nomogram M prognostic value for major adverse cardiac and cerebral events after elective cardiac surgery with cardiopulmonary bypass. *Messenger of Anesthesiology and Resuscitation*. 2022; 19(2):6–13. (In Russ.). https://doi.org/10.21292/2078-5658-2022-19-2-6-13
12. Berikashvili LB, Yadgarov MYa, Gerasimenko ON, Koger DD, Kadantseva KK, Likhvantsev VV. Risk assessment of hemodynamically significant arrhythmias after elective cardiac operations with cardiopulmonary bypass using the modified nomogram (retrospective study). *General Reanimatology*. 2021; 17(6):20–26. (In Russ.). https://doi.org/10.15360/1813-9779-2021-6-20-26
13. Biancari F, Ruggieri V, Perrotti A, Svenarud P, Dalén M, Onorati F, et al. European multicenter study on coronary artery bypass grafting (E-CABG registry): study protocol for a prospective clinical registry and proposal of classification of postoperative complications. *Journal of Cardiothoracic Surgery*. 2015; 1(10):1–12. https://doi.org/10.1186/s13019-015-0292-z
14. Nashef SA, Roques F, Sharples LD, Nilsson J, Smith C, Goldstone AR, et al. EuroSCORE II. *Eur J Cardiothorac Surg*. 2012; 41(4):734–44: discussion 744–5. https://doi.org/10.1093/ejcts/ezs043
15. Sousa-Uva M, Head SJ, Milojevic M, Collet JP, Landoni G, Castella M, et al. 2017 EACTS Guidelines on perioperative medication in adult cardiac surgery. *Eur J Cardiothorac Surg*. 2018; 53(1):5–33. https://doi.org/10.93/ejcts/ezx314. PMID: 29029110
16. Belletti A, Lerose CC, Zangrillo A, Landoni G. Vasoactive-inotropic score: evolution, clinical utility, and pitfalls. *J Cardiothorac Vasc Anesth*. 2021; 35(10):3067–3077. https://doi.org/10.1053/j.jvca.2020.09.117. PMID: 33069558
17. Khwaja A. KDIGO clinical practice guidelines for acute kidney injury. *Nephron Clin Pract*. 2012; 120(4):c179–84. https://doi.org/10.1159/000339789
18. The Lancet. ICD-11. *Lancet*. 2019 Jun 8; 393(10188):2275. https://doi.org/10.1016/S0140-6736(19)31205-X. PMID: 31180012

**Information about the authors:**

**Levan B. Berikashvili** — Research associate at Department of clinical trials of V.A. Negovsky Research Institute of General Reanimatology, Federal Research and Clinical Center of Intensive Care Medicine and Rehabilitology; Research associate at Intensive care department M.F. Vladimirsky Moscow Regional Research Clinical Institute, Moscow, Russia — **responsible for contacts**, **levan.berikashvili@mail.ru**, ORCID: 0000-0001-92673664

**Anastasiya V. Smirnova** — MD, Clinical resident of the Department of Anesthesiology and Resuscitation of First Moscow State Medical University (Sechenov University), Moscow, Russia.

**Elizaveta A. Laricheva** — MD, Clinical resident of the Department of Anesthesiology and Resuscitation of First Moscow State Medical University (Sechenov University), Moscow, Russia.

**Nadezhda D. Gracheva** — MD, Clinical resident of V.A. Negovsky Research Institute of General Reanimatology, Federal Research and Clinical Center of Intensive Care Medicine and Rehabilitology, Moscow, Russia.

**Kristina K. Kadanceva** — MD, Research associate at Department of clinical trials of V.A. Negovsky Research Institute of General Reanimatology, Federal Research and Clinical Center of Intensive Care Medicine and Rehabilitology; anaesthesiologist-resuscitator at Department of anesthesiology and resuscitation A. Loginov Moscow Clinical Scientific Center, Moscow, Russia.

**Mihail Ya. Yadgarov** — Research associate at Department of clinical trials of V.A. Negovsky Research Institute of General Reanimatology, Federal Research and Clinical Center of Intensive Care Medicine and Rehabilitology, Moscow, Russia.

**Andrey V. Grechko** — MD, ScD, Professor, Corresponding Member of the Russian Academy of Sciences, Director of the Federal Research and Clinical Center of Intensive Care Medicine and Rehabilitology, Moscow, Russia.

*The authors declare no conflicts of interest.*
*The study was not sponsored.*
*Received 11.08.2022*



# Correlations of CT signs of COVID-19 viral pneumonia with phases of diffuse alveolar damage

UDK 616-079.1
DOI: 10.53652/2782-1730-2022-3-3-38-44

**Parshin V.V.[1], Lezhnev D.A.[2], Berezhnaya E.E.[1], Mishina A.V.[2]**

*1 City Clinical Hospital No. 52, Moscow Healthcare Department, Moscow, Russia*
*[2] FSBEI HE A.I. Yevdokimov MSMSU MOH Russia, Moscow, Russia*

**Abstract.** A computed tomography (CT) is the leading diagnostic technique in identifying detailed and specific signs of coronavirus infection (CI). The objective of the work is to correlate between the typical set of signs that occur during CI and the phases of diffuse alveolar damage (DAD). The volume of lung lesions in 78 patients was retrospectively evaluated. All the patients had lung CT from 1 to 3 day before death. 14 patients had a targeted comparison of 3 signs β«ground-glass, crazy paving pattern and consolidation» with the phases of DAD. It was found that the «ground glass» feature is most characterized by the exudative phase (lasting up to 8 days), the «crazy paving pattern» βby the exudative-proliferative phase (up to 10 days), the consolidation βby the proliferative phase (lasting from 8 to 20 days). According to these scientific data, CT-lung can be a prognostic factor of histological phases of DAD and their duration, which in turn may be one of the predictors of a negative prognosis and the onset of death in pneumonia caused by SARS-CoV-2 (COVID-19).

**Keywords:** COVID-19, computed tomography of the lungs, prognostic factor, diffuse alveolar damage, histological phases.

**Introduction.** Most publications present computed tomography (CT) of the lungs as the most important diagnostic technique in detecting changes associated with viral infection (VI) [3, 6, 9-13, 15]. Obtained data on lesion volume can be considered as a predictor of patient's mortality [2].

The work by S.P. Morozov et al. who analyzed CT data of 13,003 patients, traced the probability of increased risk of fatal outcome using "CT0-4" scale [8].

Most review papers [7], as well as publications by T.N. Bilichenko [1] and E.J. Williamson et al. [14] consider the presence of comorbid pathology in a patient, such as diabetes mellitus, bronchial asthma, autoimmune, hematological and oncological diseases, combining data with age and gender. The obtained data were considered as criteria of unfavorable prognosis of the course of the disease.

In a review by the Chief Oncologist of the Ministry of Health of Russia A.D. Kaprin et al. in 2020 [5], it was specifically noted that, as of today, patients with cancer should be singled out in the group of increased risk of infection with the new coronavirus. Data on the effect of COVID-19 on cancer patients, mortality and prognosis

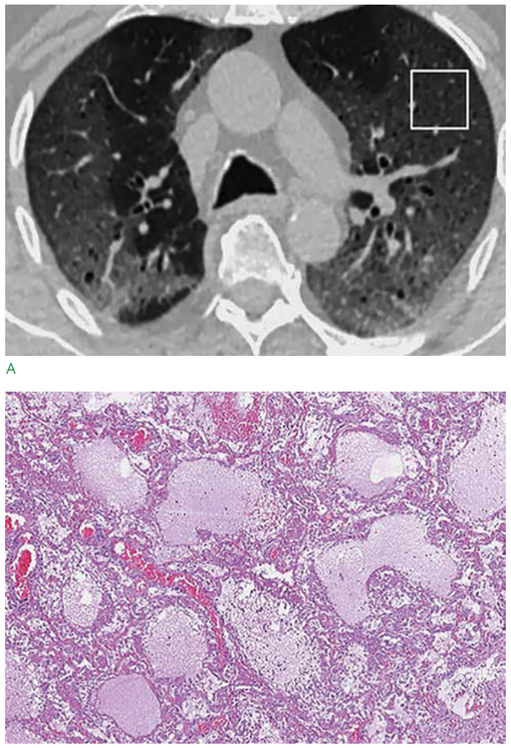

A

B

**Fig. 1.** A — Thorax CT scan, axial projection, pulmonary window mode, with a marked fragment of "ground glass" for histological analysis; B — microslide: intraalveolar edema and hyaline membranes

in COVID-19 infected patients need to be studied. All reviewed publications consider comorbid pathology and volume of lung lesions, however there are no possible options to compare histological phases of the infection course.

O.V. Zairatjants et al. [4] considered COVID-19 in terms of pathological anatomy and showed the phases of diffuse alveolar damage (DAD).

Our own data comparing CT findings with morphological signs allow us to make an attempt to reliably predict the DAP phase based on CT data. [9].

**Objective.** To analyze the correspondence of CT-signs of COVID-19 viral pneumonia with DAD phases.

**Material and methods.** The study group included 104 subjects: 59 (56.7%) men and 45 (43.3%) women with COVID-19-induced pneumonia, which had clinical manifestations and pathologically confirmed data. Computed tomography of thoracic organs was performed in 1-3 days or on the day of the patient's death, averaging 2.85±0.94 days. The mean age of all patients was 67±15.87 years.

A multispiral CT scanner Aquilion Prime (Toshiba, Japan) was used to perform lung CT: slice thickness 0.5 mm, pitch factor 1.368. The duration of the procedure did not exceed 20 s. The positioning of the patient was lying on his back with his arms raised, without contrast enhancement, followed by image reconstruction.

Image processing was performed on a workstation using standard software and MultiVox multiparametric package, which was auxiliary and allowed to quantify a group of criteria: total lesion volume of both lungs, right and left lung separately, volume of affected tissue due to 3 separate signs: "ground glass", "crazy paving pattern" and "consolidation". The signs had quantitative and percentage expression.

Autopsy was performed on all the deceased following the generally accepted technique. Lung tissue samples were taken for histological analysis from the identified and marked material according to CT scanning. The volume of the lung lesion was assessed in general and with regard to typical signs: "ground glass", "crazy paving pattern" and "consolidation". In the study group there were 26 patients with oncological diseases, and 78 of them had no previous history of oncological disease, which did not influence the pattern of the revealed changes. In 14 patients we performed targeted lung tissue sampling from CT-identified material.

Based on the detected CT changes, the target points of material sampling were selected using multiplanar reconstructions (MPR). Localization by segments and anatomical landmarks (pleura, spine, ribs) were additionally used as a reference. At autopsy the lungs were fixed entirely, without extracting them from the pleural cavities, by injecting 10% neutral formalin through the trachea at 18-20 mm aq. until they were fully expanded. After that the heart-lung complex was placed in a solution of 10% neutral formalin for 24 hours. Then each lung was dissected frontally and 1 cm thick slices were obtained. This allowed to identify the areas of altered tissue marked on the tomograms. Then 1 to 3 pieces of 2×1×0.5 cm in size were cut from the areas marked on the computer tomogram, which were embedded in paraffin and processed according to the standard technique, followed by 3–5 µm thick slices stained with hematoxylin and eosin and picrofuchsin-fuchseline.

Thus, on the one hand, we had CT-data on lung lesion volume with clear localization of the pathological process in anatomical structures, and on the other hand, we had a group of morphological criteria, which allowed to model and predict DAD phase. Statistical processing of primary data was performed using SPSS Statistics-17 program.



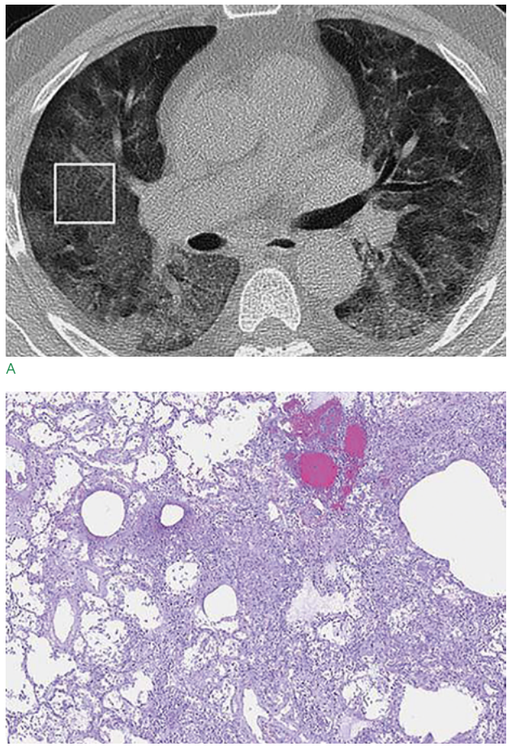

A

B

**Fig. 2.** A — Thorax CT scan, axial projection, lung window mode, targeted «crazy paving pattern» fragment for histological analysis; B — microslide: alternation of aerated and normal alveoli, intraalveolar granulation tissue, desquamated alveolocytes, focal intraalveolar hemorrhage

**Results and discussion.** It is known that histological manifestation of SARS-CoV-2-induced viral pneumonia is a DAD, proceeding in two phases: exudative and proliferative. We were interested in the following questions: what phase of DAD corresponded to the signs of "ground glass", "crazy paving pattern" and "consolidation", and whether the histological phase of the disease could be predicted by them.

Intraalveolar edema due to serous and fibrinous exudate corresponded to the "ground glass" characteristic. However, these characteristics were detected only in 28.6% of cases. In 42.9% of cases there was interstitial inflammation due to lymphoid infiltration of interalveolar septa or deposition of collagen in them (interstitial cellularity/nonspecific interstitial pneumonia (NSIP)). These changes are characteristic of the exudative phase and early proliferative phase, i.e., early manifestations of DAD are typical for "ground glass" (Fig. 1).

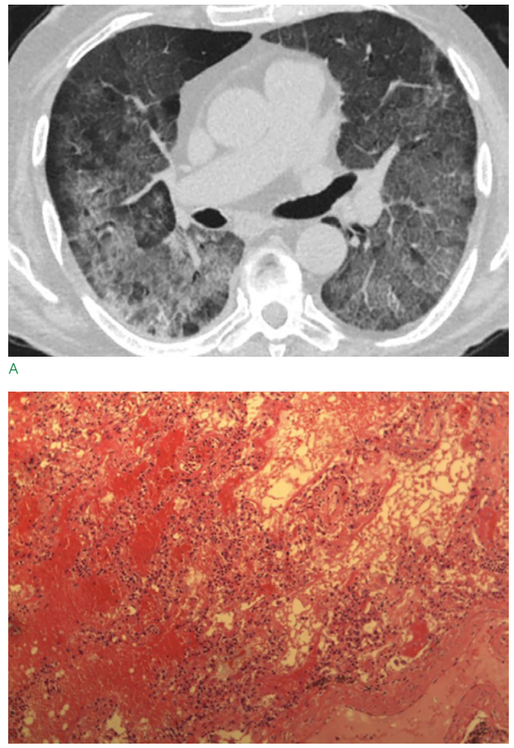

A

B

**Fig. 3.** A — Thorax CT scan, axial projection, lung window mode, targeted "crazy paving pattern" fragment for histological analysis; B — macropreparation: alternation of aerated and normal alveoli, intra-arterial granulation tissue, desquamated alveolocytes, focal intraalveolar hemorrhage are observed

Histological examination of samples from the "crazy paving pattern" area showed alternating aerated and normal alveoli, intraarterial granulation tissue, desquamated alveolocytes, and focal intraalveolar hemorrhage (Fig. 2).

Additionally, mosaic histological changes with alternation of filled alveoli (intraalveolar edema, clusters of erythrocytes, macrophages, lymphocytes, rarely neutrophils) and aerial alveoli (acute bloating or aerated alveoli) were observed in "crazy paving pattern". All these correspond to a greater extent to the exudative-proliferative phase of DAD (Fig. 3).

From the area of "consolidation" of pulmonary tissue the pathomorphological picture is represented by extensive intraalveolar hemorrhages and/or typical areas of hemorrhagic infarcts, by areas with intraalveolar fibrin accumulation and fibroplastic tissue overgrowth, which corresponds to morphological signs of organizing

pneumonia — this is already proliferative phase of DAD (Fig. 4)

Our view of the correspondence of the CT-signs: “ground glass”, “crazy paving pattern” and «consolidation» to the DAD phases is shown in Fig. 5.

“Ground glass” corresponds more to exudative or early proliferative phases; “crazy paving pattern” is more inherent to the exudative-proliferative phase, and “consolidation” to the proliferative phase. The exudative phase has a duration of 7–10 days, followed by a proliferative phase of up to 20 days.

Undoubtedly, there are no clear radiological borders and morphological signs, however, trends exist and allow to predict and state that in the presence of clinical data of viral pneumonia caused by SARS-CoV-2, CT-data of the lungs as “ground glass”, “crazy paving pattern” and “consolidation” can be predictive factors of histological phases of DAD and their duration. The exudative phase (lasting up to 8 days) is most typical for “ground glass”, the exudative-proliferative phase (up to 10 days) for “crazy paving pattern”, and the proliferative phase (lasting from 8 to 20 days) for “consolidation”.

Thus, certain CT changes in patients with COVID-19 suggest one or another phase of DAD and its duration.

**Conclusion.** After comparison of CT-data of lungs from the areas of “ground glass”, “crazy paving pattern” and “consolidation” in the presence of clinical and laboratory data of viral pneumonia caused by SARS-CoV-2, we can state that each semiotic CT-sign corresponds to certain morphological changes, which allow to assume a certain phase and duration of diffuse alveolar damage.

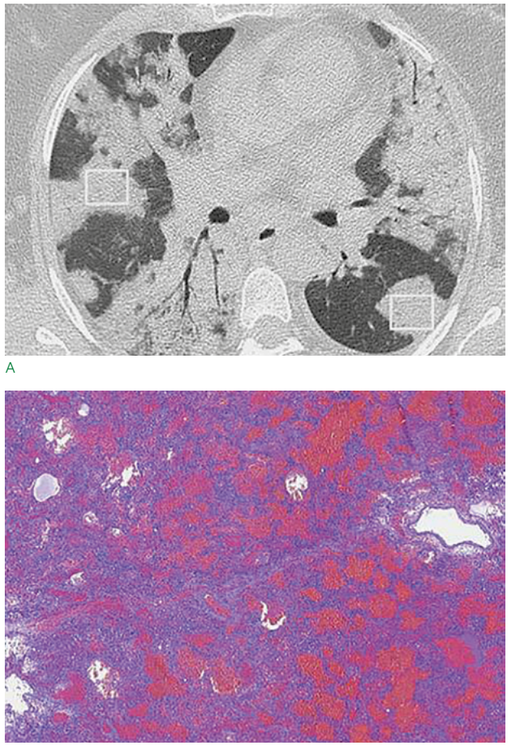

A

B

**Fig. 4.** AA — Thorax CT scan, axial projection, pulmonary window mode, marked “consolidation” fragment for histological analysis; B — microslide: massive intraalveolar hemorrhage. Hematoxylin and eosin staining

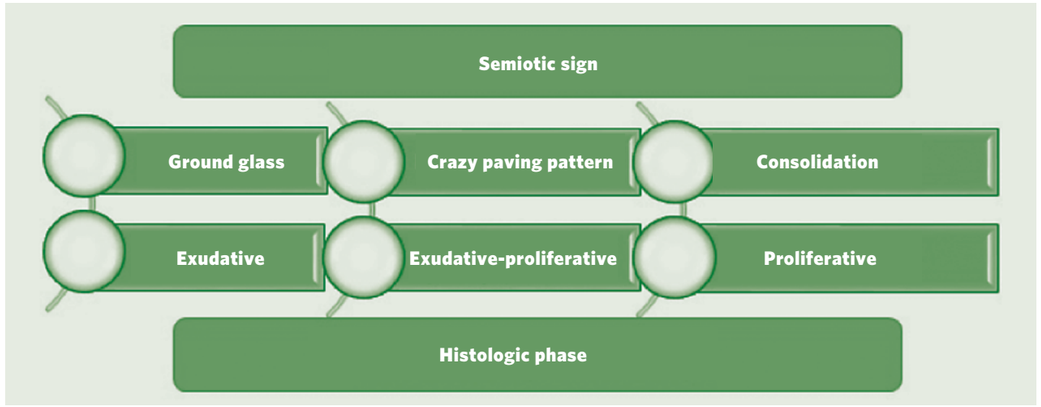


**Fig. 5.** Diagram of correspondence of CT-signs and histological phases of pneumonia caused by SARS-CoV-2 virus





## References


1. Bilichenko TN. Risk factors, immunological mechanism and biological markers of severe COVID-19 course (study overview). *Russian Medical Inquiry*. 2021; 5(5):237–244. (In Russ.). https://doi.org/10.32364/2587-6821-2021-5-5-237-244
2. Gusev AV, Novitsky RE. Predictive analytics technologies in the management of the COVID-19 pandemic. *Medical doctor and IT*. 2020; (4):24–33. (In Russ.). https://doi.org/10.37690/1811-0193-2020-4-24-33
3. Mizintseva MF, editor. *Pandemiya COVID-19. Biologiya i ekonomika*. Spetsial'nyj vypusk: informatsionno-analiticheskiy sbornik. Moscow: Pero Publ.; 2020. 110 p. (In Russ.).
4. Zayratyants OV, Samsonova MV, Mikhaleva LM, Chernyayev AL, Mishnev OD, Krupnov NM, Kalinin DV. *Patologicheskaya anatomiya COVID-19: Atlas*. Zayratyants OV, editor. Moscow: GBU «NIIOZMM DZM»; 2020. 140 p. (In Russ.).
5. Kaprin AD, Gameeva EV, Poiyakov AA, Kornietskaya AL, Rubtsova NA, Fedenko AA. Impact of the COVID-19 pandemic on the oncological practice. *Siberian Journal of Oncology*. 2020; 19(3):5–22. (In Russ.). https://doi.org/10.21294/1814-4861-2020-19-3-5-22
6. Karmazanovsky GG, Zamyatina KA, Stashkiv VI, Shantarevich MYu, Kondratyev EV, Semenov FM, et al. CT diagnostics and monitoring of the course of viral pneumonia caused by the SARS-CoV-2 virus during the work of the “COVID-19 Hospital”, based on the Federal Specialized Medical Scientific Center. *Medical Visualization*. 2020; 24(2):11–36. (In Russ.). https://doi.org/10.24835/1607-0763-2020-2-11-36
7. Molochkov AV, Karateev DE, Ogneva EYu, Zulkarnaev AB, Luchikhina EL, Makarova IV, et al. Comorbidities and predicting the outcome of COVID-19: the treatment results of 13,585 patients hospitalized in the Moscow Region. *Almanac of Clinical Medicine*. 2020; 48(Suppl 1):S1–10. (In Russ.). https://doi.org/10.18786/2072-0505-2020-48-040
8. Morozov SP, Gombolevskiy VA, Chernina VYu, Blokhin IA, Mokienko OA, Vladzimirskiy AV, et al. Prediction of lethal outcomes in COVID-19 cases based on the results chest computed tomography. *Tuberculosis and Lung Diseases*. 2020; 98(6):7–14. (In Russ.). https://doi.org/10.21292/2075-1230-2020-98-6-7-14
9. Pershina ES, Cherniaev AL, Samsonova MV, Varyasin VV, Omarova ZR, Pereshivailov SO, et al. Comparison of the CT patterns and pulmonary histology in patients with COVID-19. *Medical Visualization*. 2020; 24(3):37–53. (In Russ.). https://doi.org/10.24835/1607-0763-2020-3-37-53
10. Speranskaya AA. Radiological signs of a new coronavirus infection COVID-19. *Diagnostic Radiology and Radiotherapy*. 2020;11(1):18–25. (In Russ.). https://doi.org/10.22328/2079-5343-2020-11-1-18-25
11. Bernheim A, Mei X, Huang M, Yang Y, Fayad ZA, Zhang N, et al. Chest CT findings in coronavirus disease-19 (COVID-19): relationship to duration of infection. *Radiology*. 2020. Jun; 295(3):200463. https://doi.org/10.1148/radiol.2020200463
12. Chung M, Bernheim A, Mei X, Zhang N, Huang M, Zeng X, et al. CT Imaging Features of 2019 Novel Coronavirus (2019-nCoV). *Radiology*. 2020. Apr; 295(1):202–207. https://doi.org/10.1148/radiol.2020200230
13. Ojha V, Mani A, Pandey N, Sharma S, Kumar S. CT in coronavirus disease 2019 (COVID-19): a systematic review of chest CT findings in 4410 adult patients. *Eur Radiol*. 2020 Nov; 30(11):6129–6138. https://doi.org/10.1007/s00330-020-06975-7
14. Williamson E, Walker A, Bhaskaran K, Bacon S, Bates C, Morton CE, et al. Factors associated with COVID-19-related death using OpenSAFELY. *Nature*. 2020 Aug; 584(7821):430–436. https://doi.org/10.1038/s41586-020-2521-4
15. Ye Z, Zhang Y, Wang Y, Huang Z, Song B. Chest CT manifestations of new coronavirus disease 2019 (COVID-19): a pictorial review. *Eur Radiol*. 2020 Aug; 30(8):4381–4389. https://doi.org/10.1007/s00330-020-06801-0. PMID: 32193638



**Information about the authors:**

**Vasilij V. Parshin** — MD, Radiologist, Head of the X-ray department of City Clinical Hospital No. 52, Moscow Healthcare Department, Moscow, Russia — **responsible for contacts**, **vasilii_parshin@mail.ru,** ORCID: 0000-0003-3783-3412

**Dmitrij A. Lezhnev** — MD, ScD, Professor, Head of the Department of Radiation Diagnostics of FSBEI HE A.I. Yevdokimov MSMSU MOH Russia, Moscow, Russia.

**El'vira E. Berezhnaya** — MD, pathologist, City Clinical Hospital No. 52, Moscow Healthcare Department, Moscow, Russia.

**Anastasiya V. Mishina** — MD, PhD, Associate Professor of Phthisiology and Pulmonology Department of FSBEI HE A.I. Yevdokimov MSMSU MOH Russia, Moscow, Russia.



*The authors declare no conflicts of interest.*
*The study was not sponsored.*
*Received 10.08.2022*

# Visualization and analysis of cells with automatic counting in real time using a high-tech microscope

UDK 616-076.3
DOI: 10.53652/2782-1730-2022-3-3-45-49

**Bagrov V.V., Dikov A.V., Krylov V.I.**

*BMSTU, Moscow, Russia*

**Abstract.** An overview of a monitoring system that provides rapid, high-quality imaging with minimal preparation and allows real-time monitoring of molecular, cellular and genetic diagnostics is presented.

**Keywords:** microscope, cells, seeding, video monitoring, fluorescence, ultraviolet radiation.

**Introduction.** Life science researchers are gathering more and more information about cellular mechanisms and cell and tissue culture techniques. Understanding cell culture behavior and assessing cell health requires extensive training and experience, whereas processes such as cell subculture, growth rates, and nutritional depletion require expert understanding and optimization of these processes by trial and error. Reporting these findings is not an easy task. Personal training is ideal, but in many cases not manageable.

Cultured cells are used in various research laboratories, such as drug development, regenerative medicine and tissue engineering. A wide range of variables can affect the growth and function of cells in culture. Some of the variables cannot be managed due to their inherent stochastic processes in biological systems. However, variables such as temperature, CO2 levels, seeding density, and media components are controllable. These variables must be optimized for each cell type in order to standardize the cultivation process and obtain optimal cell growth [1].

Thus, video monitoring of cell cultures can be very useful for visual demonstration of cell culture development (Fig. 1).

**Objectives.** Application and development of an experimental model of a compact microscope (Fig. 2) for recognition of single immunological reactions previously created for the “Biotester” project as an independent device for rapid high-quality system of visualization and recognition of quantitative cell composition and identification of viable cells in the sample. Existing automated cell counters have the advantage of significantly eliminating human subjectivity from the in vitro cell counting workflow. In addition, an automated cell counter is much faster than manual counting, it can count a larger number of cells in less time (it takes only a few seconds), which increases the statistical accuracy of the experiments.

**Material and Methods.** For this work it was decided to develop a model of automatic cell counter, the basis of which was a compact inverted microscope with ultramodern optics and image analysis software based on artificial intelligence, designed for rapid cell



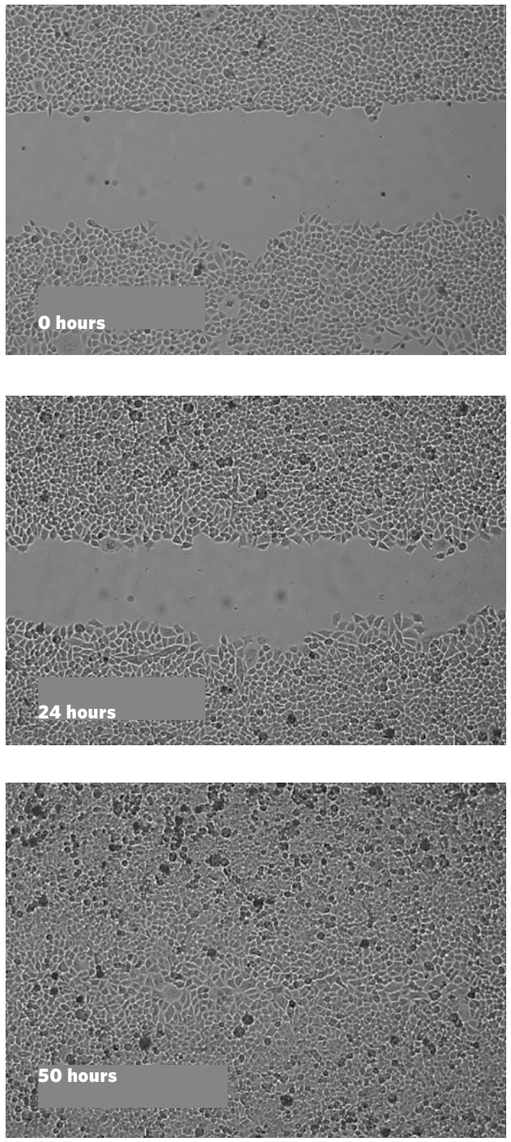


**Fig. 1.** Example of microscope analysis of cell migration for 50 h

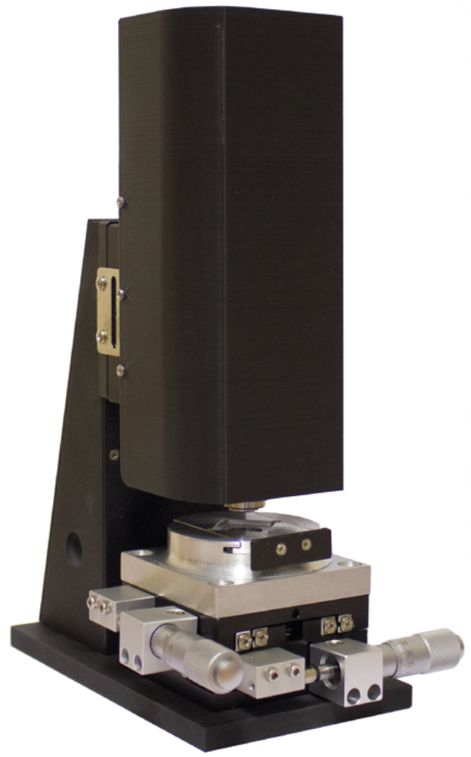

**Fig. 2.** Model of a microscope with automatic recognition of single immunological reactions

**Cultured cells are used in various research laboratories, such as drug development, regenerative medicine and tissue engineering. A wide range of variables can affect the growth and function of cells in culture. Some of the variables cannot be managed due to their inherent stochastic processes in biological systems**

counting in suspension and for obtaining bright images of live cells in any biological laboratory. The obtained images are analyzed in near real-time using dedicated image analysis software. The flexibility of the work with the three channels — light field and two additional fluorescent channels — allows researchers to quickly count cells, monitor the expression of fluorescent proteins and determine cell viability and transfection efficiency (Fig. 3) [2]. Fluorescent optical filters required for the experiments can be installed.

The use of fluorescent cell counting greatly accelerates experimental work in cancer biology, immunology, tissue engineering and cell therapy. Numerous cellular assays greatly benefit from fluorescent cell counting because of the several problems associated with detecting and analyzing mammalian cells using colorimetric dyes (e.g., trypan blue).

An instrument equipped with red and green fluorescent channels, combined with appropriate fluorescent dyes, can help in cell studies. Dyes of the PKH family (PKH2, PKH26, PKH67) are preferred for in vivo studies. This is due to the long-term retention of the mark (up to one month), which enables long-term monitoring of cell migration with high fluorescence intensity [3].

Main functions:

- modern optics allows to accurately distinguish individual cells in clusters and count cells up to 3 µm in diameter (Fig. 4);
- two-channel fluorescence can be used to examine the health and viability of hard-to-reach cells;
- Artificial intelligence-based software performs cell counting, minimizing errors between users;
- large field of view and multiple counts allow users to analyze most of the available volume;
- add-ons (e.g., organoid counting) expand the scope of the device;
- reusable or disposable counting slides to speed up and cheapen the cell counting process;
- UV exposure during the study.

The possibility of controlled UV light exposure during experiments will help in the study of cell viability in an intensive-accumulative cultivation regimen. The UVA area has a weak but diverse biological effect, causing fluorescence of organic substances; the UVB area accelerates regeneration processes, and UVC has a lethal effect on viruses and single-celled organisms, as the cause of cell death is the loss of the ability to reproduce repeatedly, which leads to loss of the cell's ability to form colonies. UV experiments will require quartz containers.

Using the automatic cell counter (Table 1), the following data can be obtained:

- the number of live and dead cells and their concentration;
- total number of cells in the sample and their concentration;

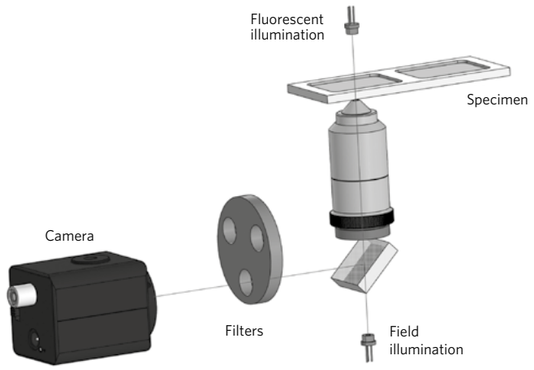


**Fig. 3.** Example diagram of an inverted microscope with three illumination channels

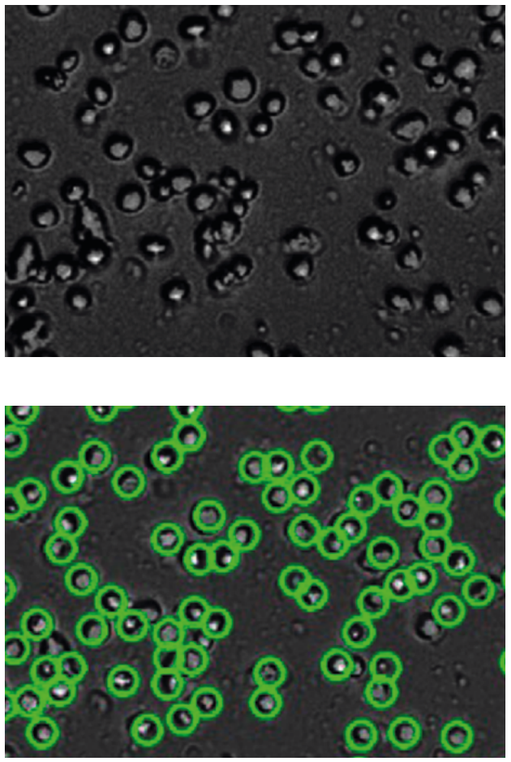

**Fig. 4.** The image analysis algorithm is able to detect clusters of cells and distinguish recognized cells

**Table 1. Technical characteristics of the automatic cell counter**

| Name | Parameters |
|---|---|
| Counting range (concentration/ml) | from $1\times10^4$ to $1\times10^7$ cells/ml |
| Particle/cell size range | 3–70 µm |
| Required sample volume | 10 µl |
| Analysis time | less than 3s |
| Fluorescent filters | Green — excitation: 452 nm; emission: 512 nm |
| Camera | Red — excitation: 561 nm; emission: 630 nm |
| Magnification | 5MP CMOS |
| Field of View | 10x lens — 20x digital |
| Cultivation vessels | 2,0×1,5 mm |
| Operating conditions | Well plates, petri dishes, flasks, microfluidic chips and special vessels for cultivation |
| Power source | Temperature: 0–42°C; humidity: 5–95% |
| | 100–240V, 2A, 50/60Hz |

- percentage of viability (percentage of live cells in relation to the total number of cells);
- images (highlighting live cells with a green line and dead cells with a red line);
- histograms of cell size distribution with the possibility of gating.

**Conclusion.** At present, the development of new technologies is accompanied by the introduction into practical healthcare of high-tech microscopes with automatic imaging systems, which allow the analysis of particles from 0.2 µm to 1600 µm in diameter, with a wide range of new parameters characterizing different cell populations, which requires analysis of their clinical relevance. It is impossible to imagine modern scientific research without process automation, providing not only saving time and expenses, but also obtaining considerably more data.

The developed microscope design can be adapted to various cell counting tasks. Its main advantage is the automatic approach to visualization and recognition, identification of viable cells and their counting. Further research will focus on improving the efficiency of the segmentation step and expanding the set of test image bases.

## References

1. Laboratornoye osnascheniye. Available at: https://www.moslabo.ru/info/cytosmart-vizualizaciya-i-analiz-zhivyh-kletok-v-realnom-vremeni/ [Accessed June 30, 2022] (In Russ.).
2. Prospekt firmy Thermo Fisher Scientific Inc., USA — 2014. Available at: https://www.dia-m.ru/upload/iblock/3f1/schetchik kletok_countess_ii_fl_therm.pdf [Accessed June 30, 2022] (In Russ.).
3. Solovieva AO, Zubareva KE, Poveschenko AF, Nechaeva EA, Konenkov VI. Methods of cells labeling for visualization in vivo. *Cell Transplantology and Tissue Engineering*. 2013; 8(4):33–38 (In Russ.). https://www.elibrary.ru/item.asp?id=21304928

**Information about the authors:**

**Valerij V. Bagrov** — PhD, Deputy Director of BMSTU, Moscow, Russia — **responsible for contacts, bagrovvv@outlook.com**, ORCID: 0000-0001-9059-6984

**Aleksandr V. Dikov** — Senior Engineer of BMSTU, Moscow, Russia.

**Vladimir I. Krylov** — PhD, Director of BMSTU, Moscow, Russia.

*The authors declare no conflicts of interest.*
*The study was not sponsored.*
*Received 06.07.2022*

# Biocompatible calcium-phosphate-collagen composite

UDK 54.057, 617, 3616.71-74
DOI: 10.53652/2782-1730-2022-3-3-50-53

**Budoragin E.S.[1], Gorshenev V.N.[2], Petcherskaya M.S.[1], Bambura M.V.[3], Dragun M.A.[4], Akopyan V.B.[4,5]**

[1] *Main Military Clinical Hospital named after academician N.N. Burdenko Russian Defense Ministry, Moscow, Russia*
[2] *Emanuel Institute of Biochemical Physics of RAS (IBCP RAS), Moscow, Russia*
[3] *Federal Institute of Industrial Property (FIPS), Moscow, Russia*
[4] *BMSTU, Moscow, Russia*
[5] *All-Russia Research Institute of Agricultural Biotechnology, Moscow, Russia*

**Abstract.** A biocompatible calcium-phosphate-collagen composite porous material, suitable for creating implants of given sizes and shapes, is synthesized accelerationally in the field of a hydroacoustic emitter, separated and conditioned in an ultrasonic self-cleaning filter. Afterwards, homogenization is performed and the obtained homogenate is used to form a body with the required size and shape, it is then exposed to lyophilic drying to form an implant, which samples sewn under the skin into the scruff of white mice for the control without causing undesirable changes in the adjacent tissues.

**Keywords:** biocomposite, biocompatibility, synthesis, ultrasound.

**Introduction.** Artificial composite structures combining mineral calcium-phosphate and polymeric organic components, as well as tissue-engineered structures in the treatment of bone tissue defects [1], are of great interest for producing biomaterials that mimic the structure and properties of natural bone tissue and are suitable for restoring the integrity of elements of the musculoskeletal system [2].

Currently, collagen-containing synthetic hydroxyapatite (HAP), a porous biocomposite that has shown in animal experiments both excellent biocompatibility and the ability to stimulate osteobiosynthesis while also acting as a matrix for the formation of new bone tissue, is in high demand to fill bone tissue defects in traumatology, maxillofacial surgery and uroplasty.

A porous composite from synthetic HAP and collagen meets the requirements of osteoplasty to a sufficient extent. Such a composite is relatively easy to standardize, and its porous structure not only facilitates fusion with the surrounding tissues but also makes it possible to load it with the drugs required in each particular case.

One of the techniques for obtaining such a biocomposite is synthesis in the field of a hydroacoustic radiator generating a wide range of frequencies in a liquid medium [3], and the use of an ultrasonic standard dispergator [4] — a source of fixed low-frequency vibrations in the range of 20-44 kHz — with sufficient power to initiate cavitation, which contributes to homogenization of a suspension of HAP with collagen. The obtained material is used to form and freeze-dry a porous structure implant with the specified size and shape.





**Experimental part.** To perform the process, aqueous solutions of the reaction ingredients are supplied to the inputs of the hydroacoustic transducer [3] at room temperature, at a pressure of 4×105 Pa, which provides cavitation at the output of the transducer. Vortex microflows with high velocity gradients significantly reduce diffusion limitations, accelerating physical and chemical interactions in a liquid medium. The use of hydroacoustic transducer makes it possible to increase the reaction speed by an order of magnitude, to obtain the target product in about 1-2 minutes and at the same time to avoid uncontrolled equipment wear, since abrasive HAP particles are formed outside the source of acoustic microcurrents.

To separate HAP particles from accidental contamination, the product from the output of hydroacoustic transducer is fed to an ultrasonic self-cleaning filter [5], where at the same time the sediment consisting of HAP particles is washed with distilled water in automatic mode.

The resulting suspension of HAP is mechanically combined with collagen and homogenized in an ultrasonic field at a frequency of 22 kHz and an energy density of 3 W/cm3 [6] for 30 s. The obtained homogenate is used to form a body with specified dimensions and shapes, and undergo freeze-drying, which results in the formation of a porous implant with specified geometric parameters. To assess the biocompatibility of the obtained material, plates of such a copolyte were sewn under the skin in the scruff of laboratory white mice, and the tissues in contact with the implant were subjected to histological examination at certain intervals.

**Results and discussion.** Preclinical tests of the composite obtained to further confirm its biocompatibility and the absence of delayed toxic effects were performed by the standard method of injecting 5×10×2 mm samples under the skin of white mice, in the area of the hackle, for a period of 2 months [6, 7, 8].

The plate implants were disinfected in the STERRAD 100NX™ system by low-temperature hydrogen peroxide (H2O2) plasma for ~50 min before being implanted under the skin of mice. The system provides guaranteed sterilization of a wide range of different materials and products without the risk of damage.

Subcutaneous implantation and subsequent histological examination of tissues localized near the implanted artificial material — calcium-phosphate biocomposites with biodegradable polymer — collagen into the scruff of laboratory white mouse showed their compatibility with tissues of a living organism. Neither inflammatory or other pathological processes in the tissues contacting with the implanted samples of calcium-phosphate-collagen composites, nor delayed toxic effects were detected (Fig. 1, 2, 3)

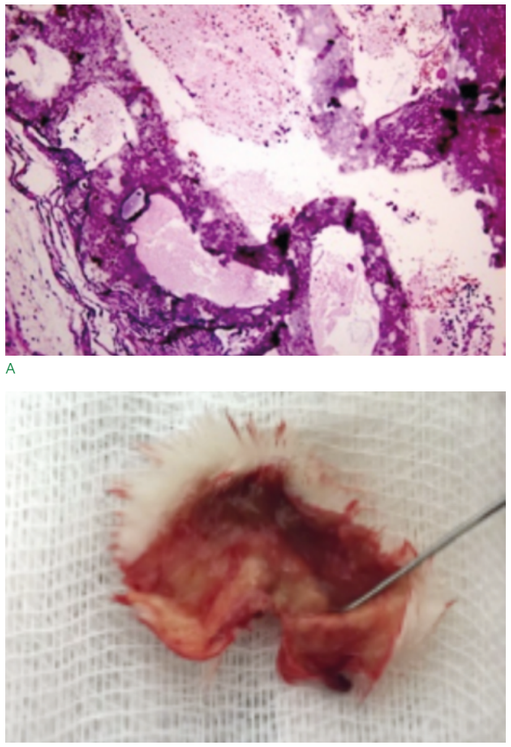

A

B

**Fig. 1.** Fragments of mouse cancellous bone with uniform, homogeneous pink substance in wide interbody spaces: A — micropreparation; B — macropreparation

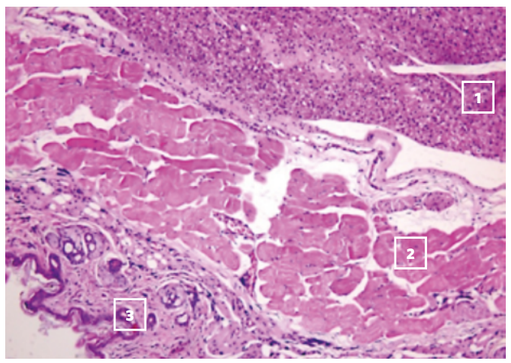


**Fig. 2.** Bone-like tissue substance with sprouting of cellular elements: 1 — elements of artificial bone; 2 — skeletal muscle tissue; 3 — skin with appendages

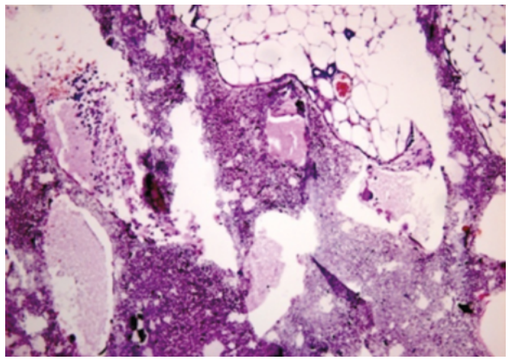

**Fig. 3.** Bone and soft tissue structures with artificial porous material (implant) without signs of rejection. No inflammatory cells were detected

**Conclusion.** Suspension of hydroxyapatite obtained by accelerated method in the field of hydroacoustic ultrasound transducer, mechanically combined with collagen in the process of homogenization by ultrasound with a frequency of 22 kHz and energy density 3 W/cm3 for 30 seconds, is promising for forming a body with given sizes and shapes with the formation after freeze-drying of biocomposite porous structure.

Subcutaneous implantation of calcium-phosphate biocomposite with biodegradable polymer - collagen in the scruff of laboratory white mice showed its biocompatibility with tissues of living organism, without delayed toxic effects, inflammatory or other pathological processes in the tissues, contacting with implanted samples.

## References


1. Kryukov EV, Brizhan' LK, Khominets VV, Davydov DV, Chirva YuV, Sevastianov VI, et al. Clinical use of scaffold-technology to manage extensive bone defects. *Orthopaedic genius.* 2019; 25(1):49–57. (In Russ.). https://doi.org/10.18019/1028-4427-2019-25-1-49-57
2. Ulery BD, Nair LS, Laurencin CT. Biomedical applications of biodegradable polymers. *J Polym Sci B Polym Phys.* 2011 Jun 15; 49(12):832–864. https://doi.org/10.1002/polb.22259. PMID: 21769165
3. Patent SU1131553A1/30.12.1984. Ponomarev VG, Smirnov VF, Sarukhanov PG, Smirnova NL. Gidrodinamicheskiy preobrazovatel'. (In Russ.). Доступно по: https://patenton.ru/patent/SU1131553A1
4. Patent RU2631594C1/25.09.2017. Gorshenev VN, Teleshev AT, Kolesov VV, Akopyan VB, Bambura MB, Budoragin YeS. Sposob polucheniya gidroksiapatit-kollagenovogo kompozita. (In Russ.). Доступно по: https://patenton.ru/patent/ RU2631594C1
5. Akopyan VB, Rukhman AA, Alenichev VV, Gavrilov VA. Intensifikatsiya protsessov fil'trovaniya. In: Proceedings of the International Conference «Ultrasonic technological processes – 2000»; Arkhangelsk, 27–30 September 2000. Arkhangelsk, 2000. pp. 28–31. (In Russ.).
6. Akopyan VB, Yershov YuA, Shchukin SI. *Ultrazvuk v meditsine, veterinarii i biologii: Uchebnoye posobiye*. Shchukin SI, editor. Moscow: Urite; 2020. 224 p. (In Russ.).
7. Oppenheimer BS, Oppenheimer ET, Danishevsky I, Stout AP, Eirich FR. Further studies of polymers as carcinogenic agents in animals. *Cancer Res.* 1955; 15(5):333–40. PMID: 14379175
8. Yastremskaya YP, Lyubchenko OD. The study of the effect of subcutaneous implantation of innovative carbon nanocomposites on antioxidant status change in the ratsβbrain. *University proceedings. Volga region.* 2015; 1(9):42–50. (In Russ.).


**Information about the authors:**


**Evgenij S. Budoragin** — Head of urological office of urological center of Main Military Clinical Hospital named after academician N.N. Burdenko Russian Defense Ministry, Moscow, Russia.

**Vladimir N. Gorshenev** — PhD in physics and mathematics, Senior research fellow at Emanuel Institute of Biochemical Physics of RAS (IBCP RAS), Moscow, Russia.

**Mariya S. Petcherskaya** — MD, pathologist, Main Military Clinical Hospital named after academician N.N. Burdenko Russian Defense Ministry, Moscow, Russia.

**Mariya V. Bambura** — PhD in Biology, state intellectual property expert, Federal Institute of Industrial Property (FIPS), Moscow, Russia.

**Maksim A. Dragun** — bachelor student in Department of Biomedical Engineering, BMSTU, Moscow, Russia.

**Valentin B. Akopyan** — ScD in Biology, professor at the Department of BMT-2 of BMSTU, Senior research fellow at All-Russia Research Institute of Agricultural Biotechnology, Moscow, Russia — **responsible for contacts**, **akopyan1941@mail.ru**, ResearcherID: A-9159-2014; eLibrary SPIN: 3265-5827



*The authors declare no conflicts of interest.*
*The study was not sponsored.*
*Received 16.08.2022*




# Modern principles of endoscopic transnasal reconstruction of skull base defects

## Literature review


UDK 616.714.3
DOI: 10.53652/2782-1730-2022-3-3-54-58



**Chernov I.V.[1], Chernov V.E.[2]**

[1] *National Medical Research Center of Neurosurgery named after academician N.N. Burdenko of the Ministry of Health of the Russian Federation, Moscow, Russia*
[2] *Main Military Clinical Hospital named after academician N.N. Burdenko Russian Defense Ministry, Moscow, Russia*



**Abstract.** Cerebrospinal fluid (CSF) leak is an urgent problem of modern neurosurgery. In elective surgery, this condition is most commonly encountered in the removal of skull base tumors. The reconstruction stage is the final stage in the course of such operations and directly affects the postoperative period of the patient. Due to advances in technology, a number of techniques that allow for hermetic closure of the intracranial space have now been developed. The most significant was the introduction of vascularized flaps, which reduced the incidence of liquorrhea many times over. This paper presents the current trends in this section of neurosurgery.



**Keywords:** CSF leak, skull base reconstruction.


**Introduction.** Nasal cerebrospinal fluid (CSF) leak in anterior cranial base defects of various etiologies is a life-threatening condition that can lead to meningitis, tension pneumocephaly, and related severe sequelae without treatment. A variety of techniques are now available to confirm liquorrhea, including analysis of the separated fluid for glucose, b-transferrin, and prostaglandin-D-synthase. Radiologic techniques are also available: CT and MR cisternography. Regardless of the cause of nasal liquorrhea (spontaneous, posttraumatic, postoperative), if conservative and minimally invasive treatment (installation of liquor draining systems) is ineffective, various surgical techniques are used, including endoscopic and endonasal. The latter has almost completely replaced the microsurgical transnasal technique over the past 20 years and significantly expanded the indications for its use [2, 3, 13, 14, 18, 26, 30, 33]. The use of extended endonasal endoscopic accesses has reduced the risk of complications inherent to transcranial surgery, associated mainly with traction of the brain and manipulation of vascular and nervous structures that are between the surgeon and pathology [19].

The most frequently encountered need for skull base defect repair is in neuro-oncology for the surgical treatment of skull base tumors. For example, in the surgery of pituitary adenomas, a worldwide experience set has identified various factors that influence the likelihood of postoperative liquorrhea, which include tumor production of somatotropic hormone, advanced age, recurrent surgery, radiotherapy, and surgical experience. However,

the discovery of an arachnoid defect and intraoperative liquorrhea are the most important factors that can increase the probability of postoperative nasal liquorrhea by 6-fold [17, 20, 30, 34]. And since intraoperative liquorrhea appears to be an imperative prognostic factor for the development of postoperative liquorrhea, cranial base defect plasty is mandatory in these cases [2, 11, 16, 17].

This paper highlights the main techniques used for the plasty of cranial base defects.

**Plasty of skull base defects with free autografts and artificial materials.** Many different techniques have been developed for plasty of skull base defects, most of which are based on the use of artificial dura mater (DM) and fibrin-thrombin glue as plastic materials [3, 4, 26, 27]. Also at the dawn of modern endoscopic transnasal surgery various free autografts were used and are still used — autografts taken from the anterior abdominal wall or the upper third of the thigh; autofascia, which can be taken from the same loci; autobones — from the nasal septum or iliac crest. Regardless of the etiology of the defect, the stages of surgery include determining the location of the defect, its skeletonization, and placement of various autografts in the defect area.

One of the most commonly used options is the "gasket seal" technique, which involves placing an autofascia in the bone defect in the projection of the DM defect with the subsequent placement of the autograft so that the latter stands tight and prevents the displacement of the autofascia. Such a plasty is reinforced with a Foley balloon catheter, installed for an average of 7 days. Lumbar drainage is also optionally used to reduce intracranial pressure for the period of healing of the defect. The effectiveness of such plastic surgery reaches 98% and depends (although not always reliably) on the initial size of the defect, the nature of the pathology, the presence of concomitant diseases (diabetes mellitus, obesity, immunodeficiency) [6, 19].

Another option for plasty of various skull base defects is the use of artificial materials, which are customized to the size and shape of the defect so as to overlap the defect by at least 5–10 mm in all directions. One of the advantages of using artificial materials is that there is no need to take your own tissues from the hip or abdomen, which improves the cosmetic results of the surgery.

**Vascularized grafts.** Conventionally, microscopic transsphenoidal surgery used fat, wide femoral fascia and sealing glue for plasty of the postoperative skull base defect. The same technique is used in endoscopic endonasal surgery [32]. However, in some cases the performed plasty turns out to be unsuccessful. This is primarily due to the fact that the plasty needs to be vascularized to perform its barrier function, which requires more time. A significant step in solving this problem was the use of mucoperiosteal (nasoseptal) flap, first described in 2006 by Hadad and Bassegastia [8, 14].

The use of vascularized tissues ensured rapid healing, which is especially important in patients undergoing radiation therapy. As a result, the use of a mucoperiosteal flap for cranial base defect plasty reduced the incidence of postoperative liquorrhea from more than 20% to less than 5% (compared with sandwich-type plasties) [11, 25].

Various flap types are currently being used.

The classical option is a flap from the nasal septum, the stem of which is located above the entrance to the choana and contains the septal branch of the sphenopalatine artery or the artery itself. To form this flap, it is necessary to make an incision of the nasal septum mucosa at the level of the natural maxillary sinus of the sphenoid bone and extend it to the vestibule of the nasal cavity. A lower incision parallel to the first one is made along the lower edge of the nasal septum, and then in the ventral parts of the nasal cavity both incisions are joined and the flap is dissected from the nasal septum. The length of such a flap is usually enough to close the defect in the posterior parts of the lattice and more caudally, including defects in the area of the sphenoid bone, the turkish saddle, and the clivus. In case of the necessity to close a wide defect the lower edge of the flap can be made along the bottom of the nasal cavity, up to its lateral parts. If it is necessary to form a particularly large flap, it is possible to make a "lower" incision of the mucosa along the lower shell and, accordingly, isolate the flap from the latter.

If the mucoperiosteal flap is inaccessible, a pericranial flap formed from the periosteum of the frontoparietal region and inserted into the nasal cavity through a small opening in the nasion area can be used. The feeding vessels of this flap are the supraorbital and supratrochlear arteries. The advantage of using this flap is its large size and primary location in the anterior parts of the anterior cranial fossa, which allows to perform reconstruction of the skull base from the ethmoid bone to the turkish saddle.

Another option is the use of a temporoparietal flap. It is formed from the fascia of the temporal muscle and the periosteum of the parietal region. To move it into the nasal cavity an endoscopic access to the infratemporal and pterygoid fossae is performed. The posterior and lateral walls of the maxillary sinus are removed, the maxillary artery and its branches are dissected. After the flap is formed, it is passed through the infratemporal fossa into the nasal cavity, and the skull base defect is repaired. The main advantage of this flap is its large size and caudo-lateral location that allows to perform plasty in the posterior parts of the ventral base of the skull, up to the inferior parts of the clivus. The use of this flap is most often the latest, in case of unsuccessful plasty with the use of all the above-mentioned options.

The use of fibrin-thrombin glue to reinforce the formed flap is considered mandatory at present. To fill the dead space between the intact bones of the skull base and the flap placed in the defect area, autograft or artificial materials (hemostatic absorbent cotton, sponge) can be used to prevent the flap from "sagging".

According to different sources, the efficacy of all the above vascularized tissues reaches 97-100% [12, 13, 23, 31], whereas the use of free and artificial tissues does not always allow to achieve similar results and is ineffective in 10-15% of cases [2-4, 6, 9, 20, 27, 32].

**Technique of suturing defects of the dura mater of the skull base.** Currently, the most promising application of the technique of suturing defects of the cranial base DM or autograft suturing. The reason for the limited use of such techniques is considered to be the difficulty of performing them in conditions of a narrow deep wound under endoscopic control. Nevertheless, the improvement of surgical skills and accumulation of experience have gradually allowed us to start using the mentioned technique, the efficiency of which is 99-100% [10, 21, 28, 29]. The use of this technique is particularly relevant for extensive defects after removal of intradural tumors of the skull base affecting the DM. Both knotty sutures and continuous sutures are used. Considering that a free graft is implanted, a vascularized flap is placed over the sutured defect to provide the best results [10].

**Discussion.** With the recent expansion of indications for endoscopic transnasal accesses in the treatment of increasingly complex pathological processes of the skull base, the problem of reconstruction of skull base defects resulting from surgical interventions has come to the forefront [24].

Previously, the high incidence of postoperative nasal liquorrhea was the main counterargument to the choice of access for the removal of skull base tumors [5]. The introduction of mucoperiosteal flap for cranial base plasty by Hadad and Bassegastia in 2006 reduced the incidence of postoperative nasal leakage to 5% and significantly expanded the indications for endoscopic transsphenoidal accesses [8, 25]. Vascularized tissues provide faster and more complete healing of skull base defects, separating the subarachnoid space from the nasal cavity and paranasal sinuses. However, retrospective analysis has shown that mortality associated with postoperative nasal liquorrhea, contrary to expectations, remains high [13]. In general, the cause is that the analysis of postoperative complications in the form of nasal liquorrhea includes all patients, including those with pituitary adenomas in which defect plasty can be performed using only free fat and autofascia. The main category of patients who develop postoperative nasal liquorrhea are those who have had chordomas, meningiomas, and craniopharyngiomas removed [18, 31].

The postoperative quality of life of the patient is also an important criterion for the choice of skull base defect plasty. For example, Pant H. et al. [22] have shown that quality of life is higher in those patients who have not undergone plasty of the skull base with a mucoperiosteal flap. This is associated with the development of such complications as cartilage necrosis, perforation of the nasal septum and impaired sense of smell [7]. In addition, Rowan et al. reported nasal dorsum fracture in the postoperative period after mucoperiosteal flap excision for skull base defect plasty [1].

**The development of techniques for the plasty of skull base defects enables to apply endoscopic technologies in the treatment of various pathologies of the skull base more and more extensively. Currently, techniques allowing reliable sealing of the subdural space even with large DM defects in 100% of cases have been developed**

It is also worth noting that the use of vascularized mucoperiosteal flaps often requires certain anatomical features of both the nasal cavity and the sphenoid sinus, which in some cases makes this method of plasty unsuitable [1, 15], which requires an individual approach to the treatment of each patient, taking into account the features of the disease and anatomy of the nasal cavity.

**Conclusion.** The development of techniques for the plasty of skull base defects enables to apply endoscopic technologies in the treatment of various pathologies of the skull base more and more extensively. Currently, techniques allowing reliable sealing of the subdural space even with large DM defects in 100% of cases have been developed.

**References**

1. Berker M, Aghayev K, Yücel T, Hazer DB, Onerci M. Management of cerebrospinal fluid leak during endoscopic pituitary surgery. *Auris Nasus Larynx*. 2013;40(4):373–8. https://doi.org/10.1016/j.anl.2012.11.006
2. Cappabianca P, Cavallo LM, Esposito F, Valente V, De Divitiis E. Sellar repair in endoscopic endonasal transsphenoidal surgery: results of 170 cases. *Neurosurgery*. 2002; 51(6):1365–71. PMID: 12445341
3. Cappabianca *P*, Cavallo LM, Valente V, Romano I, D'Enza AI, Esposito F, de Divitiis E. Sellar repair with fibrin sealant and collagen fleece

after endoscopic endonasal transsphenoidal surgery. *Surg Neurol*. 2004; 62(3):227–33. https://doi.org/10.1016/j.surneu.2004.01.016

4. Cappabianca P, Esposito F, Cavallo LM, Messina A, Solari D, di Somma LG, de Divitiis E. Use of equine collagen foil as dura mater substitute in endoscopic endonasal transsphenoidal surgery. *Surg Neurol.* 2006; 65(2):144–8. https://doi.org/10.1016/j.surneu.2005.08.023
5. Ganly I, Patel SG, Singh B, Kraus DH, Bridger PG, Cantu G, et al. Complications of craniofacial resection for malignant tumors of the skull base: report of an International Collaborative Study. *Head Neck.* 2005; 27(6):445–51. https://doi.org/10.1002/hed.20166
6. Garcia-Navarro V, Anand VK, Schwartz TH. Gasket seal closure for extended endonasal endoscopic skull base surgery: efficacy in a large case series. *World Neurosurg*. 2013; 80(5):563–8. https://*doi*.org/10.1016/j.wneu.2011.08.034
7. Greig SR, Cooper TJ, Sommer DD, Nair S, Wright ED. Objective sinonasal functional outcomes in endoscopic anterior skull-base surgery: an evidence-based review with recommendations. *Int Forum Allergy Rhinol*. 2016; 6(10):1040–1046. https://doi.org/10.1002/alr.21760
8. Hadad G, Bassagasteguy L, Carrau RL, Mataza JC, Kassam A, Snyderman CH, Mintz A. A novel reconstructive technique after endoscopic expanded endonasal approaches: vascular pedicle nasoseptal flap. *Laryngoscope*. 2006; 116(10):1882–6. https://doi.org/10.1097/01.mlg.0000234933.37779.e4
9. Harvey RJ, Parmar P, Sacks R, Zanation AM. Endoscopic skull base reconstruction of large dural defects: a systematic review of published evidence. *Laryngoscope*. 2012; 122(2):452–9. https://doi.org/10.1002/lary.22475
10. Heng L, Zhang S, Qu Y. Cross-reinforcing suturing and intranasal knotting for dural defect reconstruction during endoscopic endonasal skull base surgery. *Acta Neurochir (Wien)*. 2020; 162(10):2409–2412. https://doi.org/10.1007/s00701-020-04367-w
11. Horridge M, Jesurasa A, Olubajo F, Mirza S, Sinha S. The use of the nasoseptal flap to reduce the rate of post-operative cerebrospinal fluid leaks following endoscopic trans-sphenoidal surgery for pituitary disease. *Br J Neurosurg.* 2013; 27(6):739–41. https://doi.org/10.3109/02688697.2013.795525
12. Jalessi M, Jahanbakhshi A, Amini E, Kamrava SK, Farhadi M. Impact of nasoseptal flap elevation on sinonasal quality of life in endoscopic endonasal approach to pituitary adenomas. *Eur Arch Otorhinolaryngol.* 2016; 273(5):1199–205. https://doi.org/10.1007/s00405-0150-3729-z
13. Jeon C, Hong SD, Seol HJ, Lee JI, Nam DH, Hwang YJ, Kong DS. Reconstructive outcome of intraoperative cerebrospinal fluid leak after endoscopic endonasal surgery for tumors involving skull base. *J Clin Neurosci*. 2017; 45:227–231. https://doi.org/10.1016/j.jocn.2017.07.012
14. Kassam AB, Thomas A, Carrau RL, Snyderman CH, Vescan A, Prevedello D, et al. Endoscopic reconstruction of the cranial base using a pedicled nasoseptal flap. *Neurosurgery.* 2008; 63(1 Suppl 1):ONS44–52. https://doi.org/10.1227/01.neu.0000297074.13423.f5
15. Snyderman CH, Kassam AB, Carrau R, Mintz A. Endoscopic Reconstruction of Cranial Base Defects following Endonasal Skull Base Surgery. *Skull Base.* 2007; 17(1):73–8. https://doi.org/10.1055/s-2006-959337
16. Kelly DF, Oskouian RJ, Fineman I. Collagen sponge repair of small cerebrospinal fluid leaks obviates tissue grafts and cerebrospinal fluid diversion after pituitary surgery. *Neurosurgery.* 2001; 49(4):885–9. https://doi.org/10.1097/00006123-200110000-00020
17. Kong DS, Kim HY, Kim SH, Min JY, Nam DH, Park K, et al. Challenging reconstructive techniques for skull base defect following endoscopic endonasal approaches. *Acta Neurochir (Wien)*. 2011; 153(4):807–13. https://doi.org/10.1007/s00701-011-0941-5
18. Little RE, Taylor RJ, Miller JD, Ambrose EC, Germanwala AV, Sasaki–Adams DM, et al. Endoscopic endonasal transclival approaches: case series and outcomes for different clival regions. *J Neurol Surg B Skull Base*. 2014; 75(4):247–54. https://doi.org/10.1055/s-0034-1371522
19. Mascarenhas L, Moshel YA, Bayad F, Szentirmai O, Salek AA, Leng LZ, et al. The transplanum transtuberculum approaches for suprasellar and sellar-suprasellar lesions: avoidance of cerebrospinal fluid leak and lessons learned. *World Neurosurg*. 2014; 82(1–2):186–95. https://doi.org/10.1016/j.wneu.2013.02.032
20. Nishioka H, Haraoka J, Ikeda Y. Risk factors of cerebrospinal fluid rhinorrhea following transsphenoidal surgery. *Acta Neurochir (Wien)*. 2005; 147(11):1163–6. https://doi.org/10.1007/s00701-005-0586-3
21. Omura K, Nomura K, Mori R, Ishii Y, Aoki S, Takeda T, et al. Optimal Multiple-Layered Anterior Skull Base Reconstruction Using a 360° Suturing Technique. *Oper Neurosurg (Hagerstown)*. 2022; 22(1):e1–e6. https://doi.org/10.1227/ONS.0000000000000013
22. Pant H, Bhatki AM, Snyderman CH, Vescan AD, Carrau RL, Gardner P, et al. Quality of Life Following Endonasal Skull Base Surgery. *Skull Base*. 2010; 20(1):35–40. https://doi.org/10.1055/s-0029-1242983
23. Patel MR, Taylor RJ, Hackman TG, Germanwala AV, Sasaki–Adams D, Ewend MG, Zanation AM. Beyond the nasoseptal flap: Outcomes and pearls with secondary flaps in endoscopic endonasal skull base reconstruction. *Laryngoscope*. 2014; 124(4):846–52. https://doi.org/10.1002/lary.24319
24. Raza SM, Schwartz TH. Multi-layer reconstruction during endoscopic endonasal surgery: how much is necessary? *World Neurosurg*. 2015; 83(2):138–9. https://doi.org/10.1016/j.wneu.2014.07.004
25. Rivera–Serrano CM, Snyderman CH, Gardner P, Prevedello D, Wheless S, Kassam AB, et al. Nasoseptal "rescue" flap: a novel modification of the nasoseptal flap technique for pituitary surgery. *Laryngoscope*. 2011; 121(5):990–3. https://doi.org/10.1002/lary.21419
26. Seiler RW, Mariani L. Sellar reconstruction with resorbable vicryl patches, gelatin foam, and fibrin glue in transsphenoidal surgery: a 10-year experience with 376 patients. *J Neurosurg*. 2000; 93(5):762–5. https://doi.org/10.3171/jns.2000.93.5.0762
27. Sherman JH, Pouratian N, Okonkwo DO, Jane JA Jr, Laws ER. Reconstruction of the sellar dura in transsphenoidal surgery using an expanded polytetrafluoroethylene dural substitute. *Surg Neurol.* 2008; 69(1):73–6. https://doi.org/10.1016/j.surneu.2007.07.069
28. Shkarubo AN, Andreev DN, Chernov IV, Yegorovich SM. Surgical Correction of a Clivus Cerebrospinal Fluid Fistula: A Technical Report. *World Neurosurg*. 2021; 152:114–120. https://doi.org/10.1016/j.wneu.2021.06.061
29. Takeuchi K, Nagatani T, Wakabayashi T. How I do it: shoelace watertight dural closure in extended transsphenoidal surgery. *Acta Neurochir (Wien)*. 2015; 157(12):2089–92. https://doi.org/10.1007/s00701-015-2612-4
30. Tamasauskas A, Sinkūnas K, Draf W, Deltuva V, Matukevicius A, Rastenyte D, Vaitkus S. Management of cerebrospinal fluid leak after surgical removal of pituitary adenomas. *Medicina (Kaunas)*. 2008; 44(4):302–7. PMID: 18469507
31. Thorp BD, Sreenath SB, Ebert CS, Zanation AM. Endoscopic skull base reconstruction: a review and clinical case series of 152 vascularized flaps used for surgical skull base defects in the setting of intraoperative cerebrospinal fluid leak. *Neurosurg Focus.* 2014; 37(4):E4. https://doi.org/10.3171/2014.7.FOCUS14350
32. Wang YY, Kearney T, Gnanalingham KK. Low-grade CSF leaks in endoscopic trans-sphenoidal pituitary surgery: efficacy of a simple and fully synthetic repair with a hydrogel sealant. *Acta Neurochir (Wien)*. 2011; 153(4):815–22. https://doi.org/10.1007/s00701-010-0862-8
33. Grigor`yev AYu, Gizatullin ShKh, Chernov VE, Shitov AM, Bitner SA, Chechel` VI. Pervy`j opy`t transsfenoidal`nogo udaleniya meningiomy petroklival`noyoblasti. In: Proceedings of the VII Russian Congress of neurosurgeons; Kazan, 2–6 June 2015. P. 97. (In Russ.).
34. Shchigolev YuS, Gizatullin ShKh, Chernov VE, Antipov AB, Bogdanov-Gaydukov VV, Kurbanov SI, Glukhikh DI. Plastika dna turetskogo sedla osteomatriksom pri udalenii opukholey khiazmal`no-sellyarnoy oblasti. In: Congress proceedings of the Fifth Congress of Neurosurgeons of Russia; Ufa, 22–25 June 2009. P. 318–319. (In Russ.).

**Information about the authors:**

**Il'ya V. Chernov** — MD, neurosurgeon, National Medical Research Center of Neurosurgery named after academician N.N. Burdenko of the Ministry of Health of the Russian Federation, Moscow, Russia.

**Valerij E. Chernov** — MD, neurosurgeon, Main Military Clinical Hospital named after academician N.N. Burdenko Russian Defense Ministry, Moscow, Russia — **responsible for contacts, beduinum@rambler.ru**, ORCID 0000-0003-4882-2444

*The authors declare no conflicts of interest.*
*The study was not sponsored.*
*Received 07.06.2022*

ISSN: 2782-1730 (PRINT) / ISSN: 2713-0711 (ONLINE) / DOI:10.53652/2782-1730-2022-3-2
MEDICAL BULLETIN OF THE MAIN MILITARY CLINICAL HOSPITAL NAMED AFTER N.N. BURDENKO.
Scientific and practical edition.
Circulation 1000 copies. Format: 60—90 1/8. Sertificate of registration of mass media PI number FS77-78674 on July 10, 2020. The Bulletin is published quarterly. Signed for printing 22.09.2022.
Founder: The Main Military Clinical Hospital named after N.N. Burdenko.
Editorial board: The Main Military Clinical Hospital named after N.N. Burdenko. Gospital sq. 3105229, Moscow, Russia. Phone: +7 499 263 5555, +4509, +4512,+4513; e-mail: gvkg.300@mail.ru
The journal's articles are included in the independent database of the complete list of scientific papers — the Russian Science Citation Index (RSCI). Free access policy.
Electronic versions of the published issues of the journal are available online: hospitalburdenko.com.
Target audience: doctors of various clinical disciplines, health care organizers, doctors of related specialties, residents, postgraduates.

Journal production “Medical Bulletin of the Main Military Clinical Hospital named after N.N. Burdenko”: Publishing house “Opinion Leader”. 125183, Moscow, Likhoborskie Bugry st., 6, # 30.
Tel.: +7 926 317 4445; e-mail: opinionleaderph@gmail.com
Director of the publishing house: Anna Gurchiani. Issuing editor: Svetlana Episeeva. Design & layout: Elena Mappyrova. Photographer: Natalia Vremyachkina. Translator: Petr Radaev.